The CRISPR Journal
Volume 4, Number 5, 2021
© Mary Ann Liebert, Inc.
DOI: 10.1089/crispr.2021.0051

The CRISPR Journal

RESEARCH ARTICLE

Evolution of Type IV CRISPR-Cas Systems: Insights from CRISPR Loci in Integrative Conjugative Elements of *Acidithiobacillia*

Ana Moya-Beltrán,[1,2] Kira S. Makarova,[3] Lillian G. Acuña,[1,†] Yuri I. Wolf,[3] Paulo C. Covarrubias,[1,‡] Sergey A. Shmakov,[3] Cristian Silva,[1] Igor Tolstoy,[3] D. Barrie Johnson,[4,5] Eugene V. Koonin,[3,*] and Raquel Quatrini[1,2,6,*]

Abstract

Type IV CRISPR-Cas are a distinct variety of highly derived CRISPR-Cas systems that appear to have evolved from type III systems through the loss of the target-cleaving nuclease and partial deterioration of the large subunit of the effector complex. All known type IV CRISPR-Cas systems are encoded on plasmids, integrative and conjugative elements (ICEs), or prophages, and are thought to contribute to competition between these elements, although the mechanistic details of their function remain unknown. There is a clear parallel between the compositions and likely origin of type IV and type I systems recruited by Tn7-like transposons and mediating RNA-guided transposition. We investigated the diversity and evolutionary relationships of type IV systems, with a focus on those in *Acidithiobacillia*, where this variety of CRISPR is particularly abundant and always found on ICEs. Our analysis revealed remarkable evolutionary plasticity of type IV CRISPR-Cas systems, with adaptation and ancillary genes originating from different ancestral CRISPR-Cas varieties, and extensive gene shuffling within the type IV loci. The adaptation module and the CRISPR array apparently were lost in the type IV ancestor but were subsequently recaptured by type IV systems on several independent occasions. We demonstrate a high level of heterogeneity among the repeats with type IV CRISPR arrays, which far exceed the heterogeneity of any other known CRISPR repeats and suggest a unique adaptation mechanism. The spacers in the type IV arrays, for which protospacers could be identified, match plasmid genes, in particular those encoding the conjugation apparatus components. Both the biochemical mechanism of type IV CRISPR-Cas function and their role in the competition among mobile genetic elements remain to be investigated.

Introduction

Class 1 CRISPR/Cas systems are divided into three types (I, III, and IV), each of which is characterized by a unique signature gene.[1] The prototype of the type IV systems is the CRISPR-Cas locus of the type strain (ATCC 23270) of *Acidithiobacillus ferrooxidans*,[2] which resides in an integrative and conjugative element (ICE)[3] inserted into the chromosome of this model acidophile.[4,5] This CRISPR-Cas system has been designated AFERR, and associated genes + were named Csf (CRISPR-Cas subtype as in *A. ferrooxidans*). Currently, type IV CRISPR-Cas systems are classified into three types (A, B, and C) that have distinct characteristic operon organizations.[1] Recently, however, it has been proposed to reclassify some of these systems into new subtypes IV-D and IV-E, and to split subtype IV-A into three variants based on differences in operon organization.[6]

Similar to other class 1 CRISPR-Cas systems, all type IV systems encompass homologs of Cas5 (Csf3) and Cas7 (Csf2) key subunits of the effector complex

[1] *Fundación Ciencia y Vida, Santiago, Chile;* [2] *ANID—Millennium Science Initiative Program, Millennium Nucleus in the Biology of the Intestinal Microbiota, Santiago, Chile;* [3] *National Center for Biotechnology Information, National Library of Medicine, Bethesda, Maryland, USA;* [4] *School of Natural Sciences, Bangor University, Bangor, United Kingdom;* [5] *Faculty of Health and Life Sciences, Coventry University, Coventry, United Kingdom; and* [6] *Facultad de Medicina y Ciencia, Universidad San Sebastián, Santiago, Chile.*
[†] Current address: Laboratorio de RNAs Bacterianos, Departamento de Ciencias Biológicas, Facultad de Ciencias de la Vida, Universidad Andres Bello, Santiago, Chile.
[‡] Current address: Interdisciplinary Center for Aquaculture Research (INCAR), Universidad Andres Bello, Viña del Mar, Chile.

*Address correspondence to: *Eugene V. Koonin, PhD, National Center for Biotechnology Information, National Library of Medicine, Bethesda, MD 20894, USA,* Email: koonin@ncbi.nlm.nih.gov; *and Raquel Quatrini, PhD, Fundación Ciencia y Vida, Universidad San Sebastián, Santiago, Chile,* Email: rquatrini@cienciavida.org

involved in crRNA binding.[7,8] The originally described subtypes IV-A and IV-B share a signature protein, Csf1, that has been predicted to be structurally and functionally equivalent to the large subunits of other class 1 effector complexes, although it does not share any detectable sequence similarity with the latter and is much smaller compared to the large subunits of type I and type III systems.[9] The recently introduced subtype IV-C shares the Cas5 and Cas7 components with IV-A and IV-B, but also possesses a distinct large subunit fused to an active HD family nuclease domain, similarly to Cas10, the large subunit of type III systems. This observation led to the hypothesis on the origin of type IV systems from type III systems.[1] The signature protein of subtype IV-A systems is DinG family helicase, whereas the majority of the type IV-B loci encode a protein predicted to be a small subunit of effector complex, Cas11_IV.[1] Cas6 is encoded in most type IV-A systems, whereas in the subtype IV-B loci, *cas6* genes are scarce.[6] Subtype IV-B systems are strongly linked to *cysH* gene, the functional role of which in the context of these CRISPR-Cas systems remains unclear.[10,11] Many subtype IV-A systems include CRISPR arrays but typically lack the *cas1* and *cas2* adaptation genes and any associated nuclease that could be implicated in the target cleavage. These distinctive features imply that type IV systems do not provide adaptive immunity in the way canonical CRISPR-Cas systems can and instead could have been recruited for non-defense functions or defense functions not involving target cleavage.[11] Most type IV systems are associated with phages or plasmids and have been proposed to be involved in plasmid competition.[12,13]

Experimental data on type IV systems are scarce. Type IV CRISPR RNA (crRNA) production and maturation has been demonstrated in high-throughput RNAseq assays.[7,8] Experiments in *Escherichia coli* have shown that processing of the EbN1 pre-crRNA is mediated by the cognate type IV Cas6 and that the crRNAs are specifically incorporated into the type IV effector complex.[7,8] The Cas6 protein associated with type IV CRISPR-Cas from *Mahella australiensis* has been studied, and its structure has been solved.[14] The structure of type IV-A effector complex from *Aromatoleum aromaticum* EbN1 was partially solved, and the predicted organization of the effector complex resembling those of type I and type III effector complexes has been confirmed.[7] Most recently, a partial structure of type IV-B effector complex from *Mycobacterium* sp. JS623 type IV-B has been solved, and it has been shown that the type IV effector complex can be associated with heterogeneous small RNAs arranged in a pseudo-A-form configuration.[8] Although the functional mode of type IV CRISPR-Cas systems remains unclear, it has been shown that the system from *Pseudomonas aeruginosa* strain PA83 mediates RNA-guided interference against a plasmid *in vivo*, both clearing and inhibiting the plasmid, and a crucial role of DinG helicase in this activity has been demonstrated.[15]

Several lines of evidence provide clues to potential alternative functions of the type IV CRISPR-Cas systems distinct from adaptive immunity. Most of the type IV CRISPR-Cas systems are located on plasmids,[12] megaplasmids,[7] ICEs,[3,16] and, in several cases, prophages.[6,10,11] This trend suggests that they contribute to mobile genetic elements–host interaction, and in particular could inhibit host defense, including resident CRISPR-Cas, or contribute to the maintenance and/or enhance the mobility of plasmids via as yet unknown mechanisms.[6,10,11] Spacer target analysis of one such system partially supports this view. The IncHI1B/IncFIB plasmid-encoded type IV CRISPR from *Klebsiella* strains have been recently shown to harbor a number of spacers that match conjugational transfer genes *traN* and *traL* of IncFIIK/IncFIB(K) plasmids, suggesting a role in plasmid incompatibility.[12] In general, however, the functions of type IV CRISPR-Cas systems remain poorly understood.

Here, we explore in detail the type IV CRISPR-Cas loci in several species and strains of the *Acidithiobacillia* class[17] and reexamine the diversity, classification, and evolution of type IV systems. We demonstrate a remarkable evolutionary plasticity of type IV CRISPR-Cas, including borrowing genes from other CRISPR-Cas types and extensive shuffling of gene modules, along with the previously undetected extensive polymorphism of CRISPR repeats in type IV arrays that has no precedent in other types of CRISPR-Cas systems.

Methods

Type IV CRISPR-Cas loci

The set of genomes analyzed in this work combines sequences reported to contain previously identified type IV loci[1,6] and sequences recently added to the NCBI database from *Acidithiobacillia* class,[17] which were downloaded from NCBI FTP site (ftp://ftp.ncbi.nlm.nih.gov/genomes/all/) and are listed in Supplementary Table S1. Protein-coding genes were annotated automatically using PSI-BLAST,[18] with a 10e-4 e-value cutoff and effective database size of 2×10^7. Combined profiles from NCBI CDD database[19] and CRISPR-Cas profiles described previously[1] were used as queries. The proteins were annotated according to the best scoring match. The HHpred program was used to identify distantly related sequences for selected genes encoded in type IV loci.[20]

Additionally, CRISPRCasTyper[21] was used for the identification of Cas proteins and CRISPR-Cas system subtype assignments, and the annotation of several loci was manually adjusted according to the recently proposed classification.[6]

CRISPR array detection

CRISPR arrays were identified using the minCED tool (https://github.com/ctSkennerton/minced), which is a modification of the CRT CRISPR recognition tool[22] using default parameters. Additionally, for analysis of the *Acidithiobacillia* class arrays, the CRISPRfinder online tool was employed,[23] followed by extensive manual curation of the arrays.

Search for CRISPR protospacers

To reduce redundancy, spacers recovered from the CRISPR arrays were self-compared using BLASTN. Unique spacer sequences were analyzed using CRISPR Target[24] and used as queries in BLASTN searches against the NCBI nr nucleotide database as previously described[1] in order to identify candidate target protospacers. Hits with sequence identity >95% and query coverage >95% were retained for further analysis. Identical BLASTN hits mapping to spacer sequences in CRISPR arrays were removed. Candidate protospacer sequences mapping to intergenic versus intragenic regions were scored and analyzed in further detail.

Phylogenetic analysis

To select gene representatives, protein sequences for the selected genes were clustered with MMseqs2[25] with a sequence similarity threshold of 0.98 and a coverage threshold of 0.333. Representative sequences were aligned using MUSCLE.[26] These alignments were used as input for phylogenetic tree construction using IQ-TREE[27] with the TEST model-finder and 2,000 ultrafast bootstrap iterations. Combined FastTree[28] and UPGMA trees were built using the previously described approach.[1]

Repeat polymorphism analysis

Repeat polymorphism was estimated as the sum of the number of mismatches between a repeat and the consensus repeat sequence for each repeat in an array divided by the number of repeats. Alignments for the repeats were constructed using MAFFT[29] with the *adjustdirectionaccurately* parameter. Gaps in the alignments were not counted as mismatches and were discarded from the calculation. For each array, the repeat with the highest number of mismatches (degenerate repeat) was discarded from the calculations as well. The source data for the type IV repeats were collected from the arrays analyzed in this work, and the other CRISPR-Cas types are represented by the arrays assembled previously.[1]

Expression of the type IV CRISPR-Cas system

Fervidacidithiobacillus caldus ATCC 51756 (proposed nomenclatural emendation[17]) was cultured in mineral salts medium (MSM) with trace elements at pH 2.5 in the presence of sterile-filtered tetrathionate (5 mM) or 5 g/L of elemental sulfur. Stock solutions of tetrathionate were sterile filtered and added to the autoclaved (121°C for 15 min) MSM, whereas the finely ground ethanol-sterilized powdered sulfur was added to MSM prior to autoclaving at 105°C for 30 min. All *F. caldus* cultures were incubated at 40°C under aerobic conditions on a rotary shaker at 150 rpm. Cells were collected in the logarithmic growth phase (Log) 3 days after inoculation and at stationary phase (Stat) after 7 days. Sessile versus planktonic growth was achieved in 6 cm long and 2.5 cm diameter columns containing a 2:1 w/w mix of elemental sulfur and quartz. Mid-exponential sulfur-grown cultures were passed through the column at a continuous flow of $0.029\,m^3/(0.015\,m^2 \times 20\,seg) = 0.096\,m/s$ for 7 days. Planktonic cells were collected from flow phase and sessile cells were separated from mineral substrate by thorough washing using a solution of MSM medium and 1% sodium dodecyl sulfate (SDS) and gentle vortexing. RNA isolation, reverse transcription (RT) polymerase chain reaction (PCR), and real-time PCR were carried out following standard protocols as described by Nieto *et al.*[30] Briefly, cells were collected and re-suspended in ice-cold buffer TE (25:10), pH 8.0, with 1 × extraction buffer (per liter: 1% SDS, 50 mM Tris-HCl, pH 8.0, and 2 mM EDTA). After cell lysis, the suspensions were treated with TRIzol (Invitrogen), followed by two extractions with acid phenol and chloroform. RNA was precipitated with absolute ethanol overnight at −20°C, washed with 70% ethanol, and finally re-suspended in sterilized water. Samples were treated with DNase and purified with the Roche High Pure RNA Isolation Kit, following the manufacturer's recommendations. DNA-free high-quality RNA was stored at −80°C for downstream applications. Oligonucleotide primers used in the study are listed in Supplementary Table S2. Copy DNA (cDNA) was prepared from 3 μg total RNA using Superscript II reverse transcriptase (Thermo Fisher Scientific) according to the manufacturer's instructions. PCR products were amplified with proofreading DNA polymerase Dreamtaq (Thermo Fisher Scientific) in 25 μL reactions (1 × PCR buffer +1.5 mM $MgCl_2$) containing 30 ng template cDNA, 10 μM required primers, and 0.2 mM each deoxyribonucleotides. PCR amplification conditions were as follows: initial denaturing step at 95°C for 5 min followed by 28–30 amplification cycles (denaturation at 95°C for 30 s, annealing at the appropriate temperature depending on the specific primers pairs for 30 s, and elongation at 72°C for 1 min), and a final elongation step at 72°C for 3 min. The real-time PCR reactions were performed in the RotorGene Q PCR System (Qiagen) using the KAPA SYBR FAST qPCR Kit (Roche). The 20 μL PCR reactions contained 2 μL undiluted cDNA, 200 nM each primer, and 1 × KAPA MasterMix. The cycling protocol was as follows: initial denaturation for 10 min at 95°C followed by 40 cycles of 30 s at 95°C, 15 s at 60°C, and 30 s at 72°C. Fluorescence was measured after the extension phase at 72°C. The amplification products were subjected to a melting curve analysis, and specific amplification was confirmed by a single peak in the melting curve. The reactions for each target gene were performed in triplicate and in the same PCR run, including a no template control. Amplification efficiency was calculated from a standard curve constructed by amplifying serial dilutions of genomic DNA for each gene. These values were used to obtain the fold change in expression between conditions (sessile versus planktonic) for the genes of interest normalized against *rpoC* gene expression levels according to Nieto *et al.*[30]

Results

Comparative genomic and phylogenetic analysis of type IV loci core genes

We analyzed a data set consisting of 856 type IV loci, including 12 novel loci identified in recently sequenced genomes of *Acidithiobacillia* class species (Supplementary Tables S1 and S3). The extended loci (30 genes upstream and downstream of the type IV core genes) were automatically annotated as described in the Methods, and selected protein families were analyzed in detail using sensitive computational methods, such as PSI-BLAST and HHpred, to search for potential homologs. First, we reconstructed phylogenetic trees for representative sets of Csf2/Cas7 and Csf3/Cas5 proteins (Fig. 1 and Supplementary Fig. S1A). Because Cas7 is the most highly conserved protein among the type IV components, Cas7 phylogeny was used as the framework to classify type IV systems and explore their evolution. The signature protein families, such as Csf4/DinG (signature of subtype IV-A), putative small subunit, Cas11 (signature of subtype IV-B), and the Cas10-like large subunit (signature of subtype IV-C), CRISPR repeats, as well as typical organizations of core genes, were mapped on the Cas7 tree (Fig. 1), revealing distinct loci configurations between the major branches. It should be emphasized that, as detailed previously[1] and confirmed in the current analysis of type IV, to classify CRISPR-Cas systems unequivocally into subtypes, signature genes alone are insufficient. Multiple features, such as locus organization and presence of additional genes and CRISPR arrays, have to be taken into account, along with the phylogenies of conserved *cas* genes.

In the Cas7 tree, two of the current major subtypes, IV-A and IV-C, are monophyletic, whereas the subtype IV-B clade also includes the proposed new subtype IV-D (Fig. 1). Among the branches that have been proposed to be reclassified as new subtypes,[6] only IV-E and IV-A3 are strictly monophyletic, although most of the loci assigned to IV-A1 and IV-D also form clades. In addition, the proposed new subtype IV-E confidently groups with the IV-A branch (Fig. 1).

FIG. 1. **(A–C)** Phylogenetic analysis of Cas7 (Csf2) and comparative genomic analysis of type IV systems. Phylogenetic tree for 204 representatives of Cas7 (Csf2) shown on the left was built using the IQ-TREE method as described in the Methods. The branches are colored according to the recently proposed classification of the type IV systems.[6] Each leaf is denoted by subtype (IV-A1, IV-A2, IV-A3, IV-B, IV-C, IV-D, IV-E) as recently proposed,[6] protein identifier, and species name. Supporting values were calculated by the IQ-TREE program. Several key values supporting monophyly of type IV-A and type IV-C are highlighted in *red*. The *colored lines* behind the tree show the amended proposal for classification of these systems based on this work as follows: *green*, type IV-A; *blue*, type IV-B; and *red*, type IV-C. The phyletic pattern (presence of a gene in the type IV locus in the respective genome) is shown by *rectangles*, which are color coded according to the legend above. Representative type IV core gene neighborhoods are shown behind the patterns and color coded according to the gene designation shown for each system once. The genes and CRISPR arrays are shown to scale, and accession for respective genomic partition, species name, and coordinates of the region are indicated on the *right*. A few genes that are inserted into type IV loci are shown by *blank arrows*, with short name (if any) indicated inside the *arrow*. VIP2, ADP phosphoribosyltransferase VIP2; FlhG, MinD-like ATPase involved in chromosome partitioning or flagellar assembly; HTH, helix-turn-helix, DNA binding; TGT, queuine tRNA-ribosyltransferase. Note: To visualize the details in this figure, a 200% zoom is recommended.

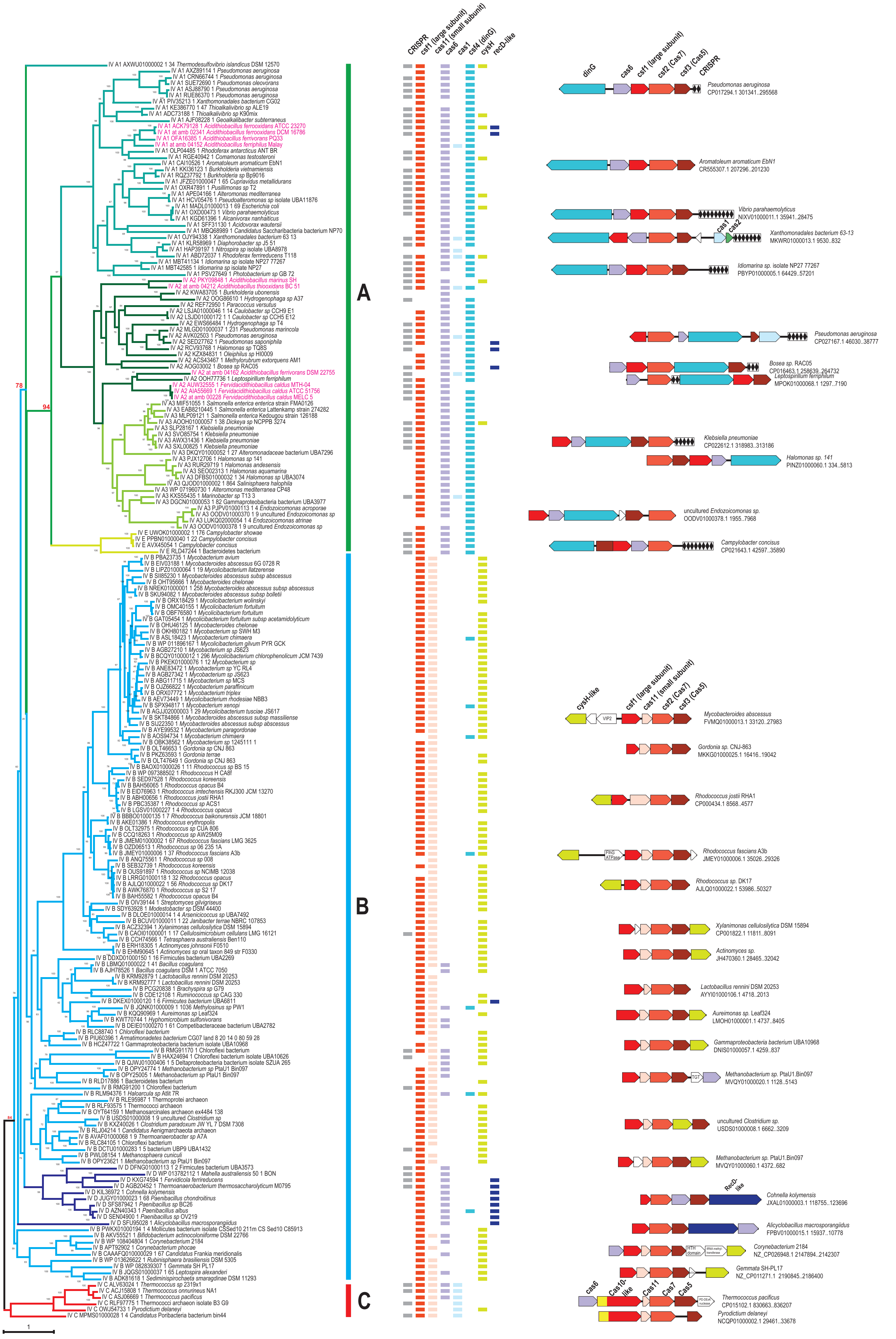
CRISPR
csf1 (large subunit)
cas11 (small subunit)
cas6
cas1
csf4 (dinG)
cysH
recD-like
78
94
84
IV A1 AXWU01000002 1 34 Thermodesulfovibrio islandicus DSM 12570
IV A1 AXZ89114 1 Pseudomonas aeruginosa
IV A1 CRN66744 1 Pseudomonas aeruginosa
IV A1 SUE72690 1 Pseudomonas oleovorans
IV A1 ASJ88790 1 Pseudomonas aeruginosa
IV A1 RUE86370 1 Pseudomonas aeruginosa
IV A1 PIV35213 1 Xanthomonadales bacterium CG02
IV A1 KE386770 1 47 Thioalkalivibrio sp ALE19
IV A1 ADC73188 1 Thioalkalivibrio sp K90mix
IV A1 AJF08228 1 Geoalkalibacter subterraneus
IV A1 ACK79128 1 Acidithiobacillus ferrooxidans ATCC 23270
IV A1 at amb 02341 Acidithiobacillus ferrooxidans DCM 16786
IV A1 OFA16385 1 Acidithiobacillus ferrivorans PQ33
IV A1 at amb 04152 Acidithiobacillus ferriphilus Malay
IV A1 OLP04485 1 Rhodoferax antarcticus ANT BR
IV A1 RGE40942 1 Comamonas testosteroni
IV A1 CAI10526 1 Aromatoleum aromaticum EbN1
IV A1 KKI36123 1 Burkholderia vietnamiensis
IV A1 RQZ37792 1 Burkholderia sp Bp9016
IV A1 JFZE01000047 1 65 Cupriavidus metallidurans
IV A1 OXR47891 1 Pusillimonas sp T2
IV A1 APE04166 1 Alteromonas mediterranea
IV A1 HCV05476 1 Pseudoalteromonas sp isolate UBA11876
IV A1 MADL01000013 1 69 Escherichia coli
IV A1 OXD00473 1 Vibrio parahaemolyticus
IV A1 KGD61396 1 Alcanivorax nanhaiticus
IV A1 SFF31130 1 Acidovorax wautersii
IV A1 MBQ68989 1 Candidatus Saccharibacteria bacterium NP70
IV A1 OJY94338 1 Xanthomonadales bacterium 63 13
IV A1 KLR58969 1 Diaphorobacter sp J5 51
IV A1 HAP39197 1 Nitrospira sp isolate UBA8978
IV A1 ABD72037 1 Rhodoferax ferrireducens T118
IV A1 MBT41134 1 Idiomarina sp isolate NP27 77267
IV A1 MBT42585 1 Idiomarina sp isolate NP27
IV A1 PSV27649 1 Photobacterium sp GB 72
IV A2 PKY09848 1 Acidithiobacillus marinus SH
IV A2 at amb 04212 Acidithiobacillus thiooxidans BC 51
IV A2 KWA83705 1 Burkholderia ubonensis
IV A2 OOG86610 1 Hydrogenophaga sp A37
IV A2 REF72950 1 Paracoccus versutus
IV A2 LSJA01000046 1 14 Caulobacter sp CCH9 E1
IV A2 LSJD01000172 1 1 Caulobacter sp CCH5 E12
IV A2 EWS66484 1 Hydrogenophaga sp T4
IV A2 MLGD01000037 1 231 Pseudomonas marincola
IV A2 AVK02503 1 Pseudomonas aeruginosa
IV A2 SED27762 1 Pseudomonas saponiphila
IV A2 RCV93768 1 Halomonas sp TQ8S
IV A2 KZX84831 1 Oleiphilus sp HI0009
IV A2 ACS43467 1 Methylorubrum extorquens AM1
IV A2 AOG03002 1 Bosea sp RAC05
IV A2 at amb 04162 Acidithiobacillus ferrivorans DSM 22755
IV A2 OOH77736 1 Leptospirillum ferriphilum
IV A2 AUW32555 1 Fervidacidithiobacillus caldus MTH-04
IV A2 AIA55669 1 Fervidacidithiobacillus caldus ATCC 51756
IV A2 at amb 00228 Fervidacidithiobacillus caldus MELC 5
IV A3 MIF51055 1 Salmonella enterica enterica strain FMA0126
IV A3 EAB8210445 1 Salmonella enterica Lattenkamp strain 274282
IV A3 MLP09121 1 Salmonella enterica Kedougou strain 126188
IV A3 AOOH01000057 1 38 Dickeya sp NCPPB 3274
IV A3 SLP28167 1 Klebsiella pneumoniae
IV A3 SVO85754 1 Klebsiella pneumoniae
IV A3 AWX31436 1 Klebsiella pneumoniae
IV A3 SXL00825 1 Klebsiella pneumoniae
IV A3 DKQY01000052 1 27 Alteromonadaceae bacterium UBA7296
IV A3 PJX12706 1 Halomonas sp 141
IV A3 RUR29719 1 Halomonas andesensis
IV A3 SEO02313 1 Halomonas aquamarina
IV A3 DFBS01000032 1 34 Halomonas sp UBA3074
IV A3 QJOD01000002 1 864 Salinisphaera halophila
IV A3 WP 071960730 1 Alteromonas mediterranea CP48
IV A3 KXS55435 1 Marinobacter sp T13 3
IV A3 DGCN01000053 1 82 Gammaproteobacteria bacterium UBA3977
IV A3 PJPV01000113 1 4 Endozoicomonas acroporae
IV A3 OODV01000370 1 9 uncultured Endozoicomonas sp
IV A3 LUKQ02000054 1 4 Endozoicomonas atrinae
IV A3 OODV01000378 1 9 uncultured Endozoicomonas sp
IV E UWOK01000002 1 176 Campylobacter showae
IV E PPBN01000040 1 22 Campylobacter concisus
IV E AVX45054 1 Campylobacter concisus
IV E RLD47244 1 Bacteroidetes bacterium
IV B PBA23735 1 Mycobacterium avium
IV B EIV03188 1 Mycobacteroides abscessus 6G 0728 R
IV B LIPZ01000064 1 19 Mycolicibacterium llatzerense
IV B SII85230 1 Mycobacteroides abscessus subsp abscessus
IV B OHT95666 1 Mycobacteroides chelonae
IV B NREK01000001 1 258 Mycobacteroides abscessus subsp abscessus
IV B SKU94082 1 Mycobacteroides abscessus subsp bolletii
IV B ORX18429 1 Mycolicibacterium wolinskyi
IV B OMC40155 1 Mycolicibacterium fortuitum
IV B OBF76580 1 Mycolicibacterium fortuitum
IV B GAT05454 1 Mycolicibacterium fortuitum subsp acetamidolyticum
IV B OHU46125 1 Mycobacteroides chelonae
IV B OKH80182 1 Mycobacterium sp SWH M3
IV B ASL18423 1 Mycobacterium chimaera
IV B WP 011896167 1 Mycolicibacterium gilvum PYR GCK
IV B AGB27210 1 Mycobacterium sp JS623
IV B BCQY01000012 1 296 Mycolicibacterium chlorophenolicum JCM 7439
IV B PKEK01000076 1 12 Mycobacterium sp
IV B ANE83472 1 Mycobacterium sp YC RL4
IV B AGB27342 1 Mycobacterium sp JS623
IV B ABG11715 1 Mycobacterium sp MCS
IV B OJZ66822 1 Mycobacterium paraffinicum
IV B ORX07772 1 Mycobacterium triplex
IV B AEV73449 1 Mycolicibacterium rhodesiae NBB3
IV B SPX94817 1 Mycobacterium xenopi
IV B AGJJ02000003 1 29 Mycolicibacterium tusciae JS617
IV B SKT84866 1 Mycobacteroides abscessus subsp massiliense
IV B SIJ22350 1 Mycobacteroides abscessus subsp abscessus
IV B AYE99532 1 Mycobacterium paragordonae
IV B AOS94734 1 Mycobacterium chimaera
IV B OBK38562 1 Mycobacterium sp 1245111 1
IV B OLT46653 1 Gordonia sp CNJ 863
IV B PKZ63593 1 Gordonia terrae
IV B OLT47649 1 Gordonia sp CNJ 863
IV B BAOX01000026 1 11 Rhodococcus sp BS 15
IV B WP 097388502 1 Rhodococcus H CA8f
IV B SED97528 1 Rhodococcus koreensis
IV B BAH56065 1 Rhodococcus opacus B4
IV B EID76963 1 Rhodococcus imtechensis RKJ300 JCM 13270
IV B ABH00656 1 Rhodococcus jostii RHA1
IV B PBC35387 1 Rhodococcus sp ACS1
IV B LGSV01000227 1 4 Rhodococcus opacus
IV B BBBO01000135 1 7 Rhodococcus baikonurensis JCM 18801
IV B AKE01386 1 Rhodococcus erythropolis
IV B OLT32975 1 Rhodococcus sp CUA 806
IV B CCQ18263 1 Rhodococcus sp AW25M09
IV B JMEM01000002 1 67 Rhodococcus fascians LMG 3625
IV B OZD06513 1 Rhodococcus sp 06 235 1A
IV B JMEY01000006 1 37 Rhodococcus fascians A3b
IV B ANQ75561 1 Rhodococcus sp 008
IV B SEB32739 1 Rhodococcus koreensis
IV B OUS91897 1 Rhodococcus sp NCIMB 12038
IV B LRRG01000118 1 32 Rhodococcus opacus
IV B AJLQ01000022 1 56 Rhodococcus sp DK17
IV B AWK76870 1 Rhodococcus sp S2 17
IV B BAH55582 1 Rhodococcus opacus B4
IV B OIV39144 1 Streptomyces gilvigriseus
IV B SDY63928 1 Modestobacter sp DSM 44400
IV B DLOE01000014 1 4 Arsenicicoccus sp UBA7492
IV B BCUV01000011 1 22 Janibacter terrae NBRC 107853
IV B ACZ32394 1 Xylanimonas cellulosilytica DSM 15894
IV B CAOI01000001 1 17 Cellulosimicrobium cellulans LMG 16121
IV B CCH74566 1 Tetrasphaera australiensis Ben110
IV B ERH18305 1 Actinomyces johnsonii F0510
IV B EHM90645 1 Actinomyces sp oral taxon 849 str F0330
IV B DDXD01000150 1 16 Firmicutes bacterium UBA2269
IV B LBMQ01000022 1 41 Bacillus coagulans
IV B AJH78526 1 Bacillus coagulans DSM 1 ATCC 7050
IV B KRM92879 1 Lactobacillus rennini DSM 20253
IV B KRM92777 1 Lactobacillus rennini DSM 20253
IV B PCG20838 1 Brachyspira sp G79
IV B CDE12108 1 Ruminococcus sp CAG 330
IV B DKEX01000120 1 6 Firmicutes bacterium UBA6811
IV B JQNK01000009 1 1036 Methylosinus sp PW1
IV B KQQ90969 1 Aureimonas sp Leaf324
IV B KWT70744 1 Hyphomicrobium sulfonivorans
IV B DEIE01000270 1 61 Competibacteraceae bacterium UBA2782
IV B RLC88740 1 Chloroflexi bacterium
IV B PIU60396 1 Armatimonadetes bacterium CG07 land 8 20 14 0 80 59 28
IV B HCZ47722 1 Gammaproteobacteria bacterium isolate UBA10968
IV B RMG91170 1 Chloroflexi bacterium
IV B HAX24694 1 Chloroflexi bacterium isolate UBA10626
IV B QJWJ01000406 1 5 Deltaproteobacteria bacterium isolate SZUA 265
IV B OPY24774 1 Methanobacterium sp PtaU1 Bin097
IV B OPY25005 1 Methanobacterium sp PtaU1 Bin097
IV B RLD17886 1 Bacteroidetes bacterium
IV B RMG91200 1 Chloroflexi bacterium
IV B RLM94376 1 Haloarcula sp Atlit 7R
IV B RLE95987 1 Thermoprotei archaeon
IV B RLF93575 1 Thermococci archaeon
IV B OYT64159 1 Methanosarcinales archaeon ex4484 138
IV B USDS01000008 1 9 uncultured Clostridium sp
IV B KXZ40026 1 Clostridium paradoxum JW YL 7 DSM 7308
IV B RLJ04214 1 Candidatus Aenigmarchaeota archaeon
IV B AVAF01000068 1 9 Thermoanaerobacter sp A7A
IV B RLC84105 1 Chloroflexi bacterium
IV B DCTU01000283 1 5 bacterium UBP9 UBA1432
IV B PWL08154 1 Methanosphaera cuniculi
IV B OPY23621 1 Methanobacterium sp PtaU1 Bin097
IV D DFNG01000113 1 2 Firmicutes bacterium UBA3573
IV D WP 013782112 1 Mahella australiensis 50 1 BON
IV D KXG74594 1 Fervidicola ferrireducens
IV D AGB20452 1 Thermoanaerobacterium thermosaccharolyticum M0795
IV D KIL36972 1 Cohnella kolymensis
IV D JUGY01000023 1 68 Paenibacillus chondroitinus
IV D SFS87942 1 Paenibacillus sp BC26
IV D AZN40343 1 Paenibacillus albus
IV D SEN04900 1 Paenibacillus sp OV219
IV D SFU95028 1 Alicyclobacillus macrosporangiidus
IV B PWKX01000194 1 4 Mollicutes bacterium isolate CSSed10 211m CS Sed10 C85913
IV B AKV55521 1 Bifidobacterium actinocoloniiforme DSM 22766
IV B WP 108404804 1 Corynebacterium 2184
IV B APT92902 1 Corynebacterium phocae
IV B CAAAFQ010000029 1 67 Candidatus Frankia meridionalis
IV B WP 013626622 1 Rubinisphaera brasiliensis DSM 5305
IV B WP 082839307 1 Gemmata SH PL17
IV B JQGS01000037 1 65 Leptospira alexanderi
IV B ADK81618 1 Sediminispirochaeta smaragdinae DSM 11293
IV C ALV63024 1 Thermococcus sp 2319x1
IV C ACJ15808 1 Thermococcus onnurineus NA1
IV C ASJ06669 1 Thermococcus pacificus
IV C RLF97775 1 Thermococci archaeon isolate B3 G9
IV C OWJ54733 1 Pyrodictium delaneyi
IV C MPMS01000028 1 4 Candidatus Poribacteria bacterium bin44
1
A
B
C
dinG
cas6
csf1 (large subunit)
csf2 (Cas7)
csf3 (Cas5)
CRISPR
Pseudomonas aeruginosa
CP017294.1 301341..295568
Aromatoleum aromaticum EbN1
CR555307.1 207296..201230
Vibrio parahaemolyticus
NIXV01000011.1 35941..28475
cas1
cas2
Xanthomonadales bacterium 63-13
MKWR01000013.1 9530..832
Idiomarina sp. isolate NP27 77267
PBYP01000005.1 64429..57201
Pseudomonas aeruginosa
CP027167.1 46030..38777
Bosea sp. RAC05
CP016463.1 258639..264732
Leptospirillum ferriphilum
MPOK01000068.1 1297..7190
Klebsiella pneumoniae
CP022612.1 318983..313186
Halomonas sp. 141
PINZ01000060.1 334..5813
uncultured Endozoicomonas sp.
OODV01000378.1 1955..7968
Campylobacter concisus
CP021643.1 42597..35890
cysH-like
csf1 (large subunit)
cas11 (small subunit)
csf2 (Cas7)
csf3 (Cas5)
VIP2
Mycobacteroides abscessus
FVMQ01000013.1 33120..27983
Gordonia sp. CNJ-863
MKKG01000025.1 16416..19042
Rhodococcus jostii RHA1
CP000434.1 8568..4577
FlhG ATPase
Rhodococcus fascians A3b
JMEY01000006.1 35026..29326
Rhodococcus sp. DK17
AJLQ01000022.1 53986..50327
Xylanimonas cellulosilytica DSM 15894
CP001822.1 11811..8091
Actinomyces sp.
JH470360.1 28465..32042
Lactobacillus rennini DSM 20253
AYYI01000106.1 4718..2013
Aureimonas sp. Leaf324
LMOH01000001.1 4737..8405
Gammaproteobacteria bacterium UBA10968
DNIS01000057.1 4259..837
TGT
Methanobacterium sp. PtaU1.Bin097
MVQY01000020.1 1128..5143
uncultured Clostridium sp.
USDS01000008.1 6662..3209
Methanobacterium sp. PtaU1.Bin097
MVQY01000060.1 4372..682
RecD-like
Cohnella kolymensis
JXAL01000003.1 118755..123696
Alicyclobacillus macrosporangiidus
FPBV01000015.1 15937..10778
HTH domain
tRNA methyl-transferase
Corynebacterium 2184
NZ_CP026948.1 2147894..2142307
HTH
Gemmata SH-PL17
NZ_CP011271.1 2190845..2186400
cas6
Cas10-like
Cas11
Cas7
Cas5
PD-DExK nuclease
Thermococcus pacificus
CP015102.1 830663..836207
Pyrodictium delaneyi
NCQP01000002.1 29461..33678

In the phylogeny of Cas5, a protein that is less strongly conserved at the sequence level than Cas7, none of the major subtypes are monophyletic (although in subtypes A and C, there are only a few outliers), whereas among the proposed new subtypes and variants, E and A3 are monophyletic (Supplementary Fig. S1A). In this tree, the proposed subtype D clearly splits into two clades, one of which falls within the subtype A clade, whereas the other one groups with the proposed subtype IV-E (with support values >70%). Another example of potential gene shuffling is the confident placement of subtype IV-C Cas5 from the *Candidatus Poribacteria* bacterium within the IV-B branch (Fig. 1 and Supplementary Fig. S1A).

Putative large subunits (Csf1-like and Cas10-like subunits of type IV-C systems) associated with type IV systems are highly diverse and are often difficult to identify. In the previous analysis by Pinilla-Redondo *et al.*,[6] the large subunit has not been identified in the proposed IV-A2 group, which was one of the criteria for making this group a separate variant. Using both PSI-BLAST and HHpred, we were able to identify this subunit, which is encoded divergently to the *csf2* gene (Cas7), in all proposed IV-A2 systems (Fig. 1 and Supplementary Fig. S2). To analyze the relationships between the large subunits, we built a dendrogram using a combination of HHalign scores and the standard phylogenetic approach employed for clusters with alignable sequences (Supplementary Fig. S1B). None of the major subtypes—A, B, and C—formed clades in the resulting tree, although the newly proposed subtype E and the variant A3 did. Similar to the Cas5 tree, the proposed subtype D split into two branches with apparently different origins, but both with affinity to Csf1-like proteins from subtype B. Our analysis therefore indicates that the large subunit sequences of the proposed variant A1 and subtype D group together with the homologous sequences of subtype B, whereas most of the Csf1-like proteins of the proposed variants A2 and A3 are similar to each other but distant from A1 (Supplementary Fig. S1B). There are also smaller branches in this tree, which correspond to highly diverged variants of Csf1 (Supplementary Fig. S1B). Most likely, this can be explained by differences in the evolutionary rates of *csf1*-like genes in different groups. Also, as in the case of the Cas5 component, these observations suggest that different genes in the proposed subtype IV-D have different origins, making these loci hybrid.

In agreement with previous observations, putative small subunits were identified in the vast majority of type IV-B systems and in all IV-C systems but not in any of the type IV-A systems (Fig. 1 and Supplementary Table S3). Despite the confident placement of both Cas7 and Csf1 components of the proposed subtype IV-D within the IV-B clade, no putative small subunits were detected in the IV-D loci.

In accordance with the previous phylogenetic analysis of Cas6,[6] we observed a remarkable diversity of *cas6* genes associated with type IV loci. There are at least six major clades of Cas6 encoded in these loci and several smaller clades that include diverged Cas6 variants (Supplementary Fig. S3 and Table S3). Only subtypes type IV-C and the proposed subtype IV-E and variant IV-A3 were monophyletic in the Cas6 phylogeny (Supplementary Fig. S3). These observations imply a complex evolutionary history of Cas6 in type IV systems, following the apparent loss of Cas6 at the onset of type IV evolution (see discussion below).

Generally, type IV loci are evolutionarily labile, with many cases of apparent gene shuffling, inversions, and insertions of various genes next to different *cas* genes such that these genes might be co-transcribed with the *cas* genes in the respective loci (Fig. 1 and Supplementary Table S3).

In addition to the genes encoding the effector complex subunits and *cas6* genes, some type IV loci, mostly of the IV-A subtype, include the adaptation genes *cas1* and *cas2*. Here, we also analyzed Cas1 sequences from type IV loci and identified two distinct phylogenetic affinities of these genes, one with subtype I-E and the other (only in *Pseudomonas* species) with I-F (Supplementary Fig. S4), which is also consistent with the analysis of CRISPR repeats in the type IV loci.[6] These findings suggest two independent acquisitions of adaptation module genes during the evolution of type IV systems. Considering the patchy distribution of Cas1 in type IV loci along with the apparent origin of the type IV-associated *cas1* genes from a distinct clade within subtype I-E, the provenance of the type IV adaptation modules can be explained either by multiple independent losses of ancestral Cas1 or, more likely, by secondary acquisitions and multiple recombination events between type IV loci (Fig. 1).

Acidithiobacillia class type IV systems are diverse and belong to four distinct groups (named after the most abundant species representative) as apparent from both the Cas7 and Cas5 phylogenies. The Caldus group, encompassing the loci from *F. caldus* strains and the Ferrivorans group represented by *Acidithiobacillus ferrivorans* DSM 22755^T single loci, are close to one another in both these trees (Figs. 1 and 2 and Supplementary Fig. S1A). Type IV CRISPR-Cas systems in these groups show considerable differences with respect to the arrangement of the core genes as well as the location and

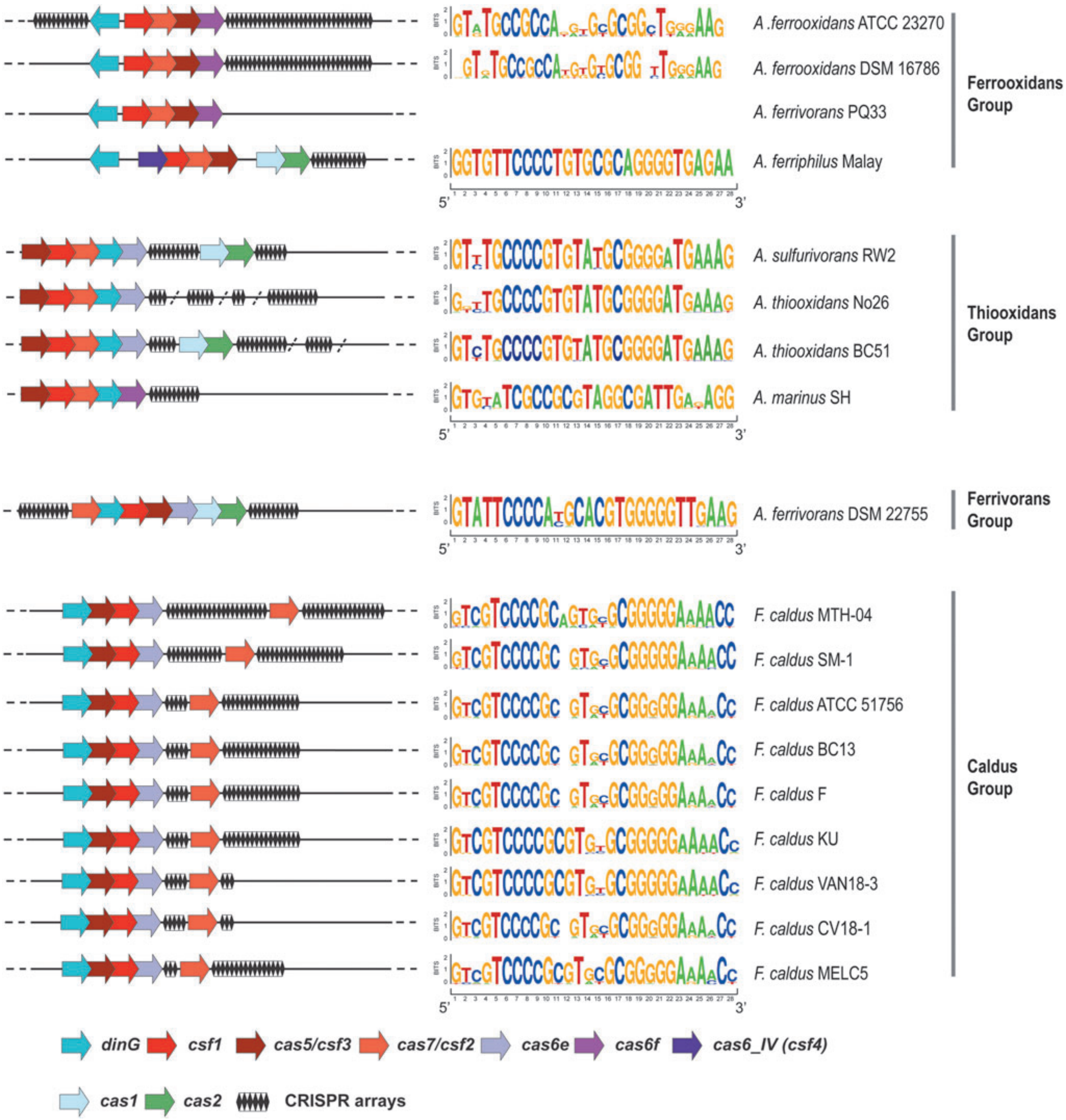

FIG. 2. Schematic representation of the diversity of type IV CRISPR-Cas systems in *Acidithiobacillia* class species and strains. The core type IV-A genes are shown by *arrows*, and CRISPR arrays are shown as *diamonds*. The genes are not shown to scale. On the *right side*, the Seqlogos (constructed using WebLogo interface https://weblogo.berkeley.edu/logo.cgi) of the repeats in all arrays in the respective type IV-locus are shown. CRISPR arrays found elsewhere in the genome or in unassembled contigs are separated by a *slash*.

size of the CRISPR arrays (Fig. 2). Moreover, even within one group, we observed extensive gene shuffling within the type IV loci. For example, the order of the *cas* genes in *Acidithiobacillus ferriphilus* Malay differs from that in the other strains in the Ferrooxidans group. Furthermore, the Cas1–Cas2 module is present in some loci but not in others. Considering that most of the *cas1* genes from these loci belong to the same branch in the Cas1 phylogeny, it appears that the adaptation module is exchanged among the type IV loci (Fig. 2 and Supplementary Fig. S4). The exception is the Cas1 from *A. ferriphilus* Malay, which is the deepest branch in the IV-A Cas1 subtree (Supplementary Fig. S4). Interestingly, the CRISPR array in this strain is the only one in type IV systems that contains identical repeats (see below; Fig. 2). Apart from gene shuffling, the evolution of type IV system in the *Acidithiobacillia* was apparently affected by changes in evolutionary rates that might correspond to functional shifts. Thus, type IV loci from the Thiooxidans group encode a highly divergent Csf1 protein, suggesting rapid evolution of this gene (Fig. 2 and Supplementary Fig. S1B).

Genes tightly associated with type IV loci

As noticed previously, in addition to the effector complex genes, most of the subtype IV-A loci encode the DinG helicase, which is the signature of this subtype. This association was confirmed in the present analysis (Fig. 1), and indeed, it has been shown that DinG is necessary for interference against plasmids.[15]

The *cysH*-like genes that have been identified in many neighborhoods of type IV-B loci are less stably associated with the IV-B systems but are often also present in the vicinity of type IV-A systems (Fig. 1). The CysH-like proteins are members of the adenine nucleotide alpha hydrolase family, which includes homologs of 3′-phosphoadenosine-5′-phosphosulfate (PAPS)-reductase, the key enzyme of the sulfate-assimilation pathway and cysteine biosynthesis, N-type ATP PPases, and ATP sulfurilases.[31] These enzymes are also components of the antiphage defense DNA phosphorothioation system[32,33] and, furthermore, are also found in some phages and are thought to facilitate inorganic sulphate assimilation by their bacterial hosts.[34–36]

We constructed a phylogenetic tree of CysH-like proteins and reproduced our previous observations[10] that CysH-like genes associated with subtype IV-B loci are largely monophyletic, but those found in the extended subtype IV-A loci are not (Supplementary Fig. S5A and Table S3). We also found that these proteins belong to a large clade that consists of CysH-like proteins that are typically encoded in mobile genetic elements (MGE), such as plasmids, phages, and other integrated elements, unlike the *bona fide* CysH (APS/PAPS reductase), which is involved in sulfate assimilation and forms a compact clade in the CysH tree (Supplementary Fig. S5A). Examination of the multiple alignment shows that unlike APS/PAPS reductases, most of the CysH-like proteins in this clade, including all those associated with type IV CRISPR-Cas, contain the sulfonucleotide-binding domain but lack the conserved cysteine of the active site in the C-terminal catalytic domain of the reductase (Supplementary Fig. S6).[37] Thus, the type IV associated CysH-like proteins, as well as most of the other proteins in this clade, are not PAPS reductases but rather, most likely, sulfonucleotide-binding proteins. Similar observations have been recently published by Taylor *et al.*,[38] who hypothesized that the role of the CysH-like protein in type IV systems is to stabilize the AMPylation of specific substrates through the ATP α-hydrolase activity. The actual activities and functions of the CysH-like proteins in plasmids and other MGE remain to be studied experimentally.

Another gene of interest is the RecD homolog that has been suggested as a signature for the proposed subtype IV-D.[6] Indeed, this gene is found in the predicted operons of all these systems, although it is often present also within extended loci of many other type IV systems (Fig. 1 and Supplementary Tables S1 and S3). As in all of the Cas protein trees discussed above, apart from Cas7, the proposed subtype D is not monophyletic in the RecD family tree, suggesting at least three independent incorporations of the *recD* gene into the respective type IV operons (Supplementary Fig. S5B). Similar to CysH homologs, RecD homologs that are encoded in the type IV loci belong to a distinct clade enriched in proteins encoded in MGE, as opposed to another major clade that consists of *bona fide* bacterial RecD helicases, components of the exonuclease V DNA repair complex RecBCD. Furthermore, the plasmid relaxase TraA,[39] a RecD homolog, belongs to the same clade as the RecD homologs from type IV loci (Supplementary Fig. S5B). The nature of the functional link between RecD and type IV systems, if any, remains obscure. However, it cannot be ruled out that RecD continues to function as a plasmid relaxase and is associated with type IV systems, since both genes are transcribed at the same time during the plasmid life cycle, a phenomenon known as gene hitch-hiking.[40]

Extended neighborhoods of type IV effector genes

Analysis of extended surroundings of type IV core genes revealed little conservation. This is not surprising, considering that type IV systems are encoded on a variety of plasmids, prophages, and other integrated elements as well as at least one phage, bacteriophage SPI1 from *Skermania piniformis*.[41] All these MGE are enriched in poorly conserved and fast-evolving genes. Indeed, search of the neighboring gene products for domains from the pfam, COGs, CDD, or Cas database showed a sharp drop in the density of detected domains outside of the type IV loci core and the tightly associated genes, such as *cysH* (Supplementary Fig. S7). These searches detected primarily genes that are typical of MGE, such as *parA* and *parB* involved in plasmid partitioning[42] and *xerD*-like integrases (Table 1).[43] Analysis of tighter gene clusters (MMseq identity threshold 0.5) yielded an overlapping but distinct set, dominated by functionally characterized genes (Table 1). The two most abundant protein families in this list, namely Vip2-like ADP phosphoribosyltransferase (e.g., EIV03191.1) and an uncharacterized protein family (e.g., EIV03192.1), have been identified in our previous analysis of genes linked to CRISPR loci.[10] Both protein sets included a MoxR-like ATPase that has been recently described as a hub in a network of functional systems implicated in various biological conflicts.[44] Specifically, a three-component module that, in addition to MoxR includes a Zincin superfamily metallopeptidase fused to a vWA domain (e.g., OHT95645.1) and a putative toxin precursor (e.g., OHT95646.1), is most often present in the vicinity of type IV loci. Generally, however, the type IV loci are found in ''dark matter'' islands, such that the neighboring genes are present in only a few other islands, suggesting that these loci are prone to frequent gene shuffling and are not essential for the propagation of the respective MGE, but rather are more or less random clusters of genes involved in anti-defense functions and inter-MGE competition (Supplementary Table S3).

Table 1. Protein Families Most Often Encoded in the Extended Gene Type IV Neighborhoods

Cluster/ family ID	*Weighted frequency*	*Comment*
MMseq 0.5 clusters		
CLUSTER_52	28.7	CysH-like
CLUSTER_53	28.7	ADP phosphoribosyltransferase VIP2-like
CLUSTER_28	22.3	MoxR-like ATPase
CLUSTER_141	21.3	Unknown
CLUSTER_40	19.4	MoxR associated zincin metallopeptidase fused vWFA domain
CLUSTER_33	18.8	DNA2-like Helicase
CLUSTER_256	13.7	Uncharacterized DUF1870
CLUSTER_46	13.4	CysH-like
CLUSTER_119	11.8	MoxR associated (precursor releasing small C-terminal peptide)
CLUSTER_126	9.4	MoxR associated (precursor releasing small C-terminal peptide)
CDD assignments		
COG0175	103.17	CysH-like
COG1199	76.0	DinG
COG1674	33.5	DNA segregation ATPase FtsK/SpoIIIE
COG1396	30.7	XRE-family HTH domain
COG4974	29.7	Site-specific recombinase XerD
COG1475	27.9	Chromosome segregation protein Spo0J, contains ParB-like nuclease domain
COG0714	26.7	MoxR-like ATPase
COG1192	24.4	Chromosome segregation ATPase ParA
COG2801	24.0	Transposase InsO
COG1028	24.0	NAD(P)-dependent dehydrogenase
cd00093	23.3	Helix-turn-helix XRE-family like proteins.
COG0582	20.7	Site-specific recombinase XerC
pfam07510	20.5	Protein of unknown function (DUF1524), predicted His-Me finger endonuclease
COG3864	20.4	Zincin metal-dependent peptidase, MoxR associated

Comparison of type IV CRISPR-Cas loci in Acidithiobacillia *class species*

As indicated by the presence of characteristic genes of the type 4 conjugative transfer system (e.g., *virB4*, *trb*, and *tra* genes), all type IV CRISPR-Cas loci in *Acidithiobacillia* class species are located in ICEs on the bacterial chromosome (Fig. 2 and Supplementary Table S3).[45–48] In *A. ferrooxidans* ATCC 23270^{T}, the type IV locus occurs in ICE*Afe*1, a well-characterized ICE,[3,43,45] whereas in *F. caldus* ATCC 51756^{T} it occurs within the ICE*Aca*1.2.[16] Both ICEs are large (183–291 Kbp) and have been shown to be stably inherited and actively excised from the chromosome in response to DNA damage, and are likely prone to conjugative transfer. While ICE*Afe*1 is poorly conserved in *Acidithiobacillus* species and strains, ICE*Aca*1.2 occurs in other *F. caldus* strains.[45,49] The Caldus group is the largest and best represented among the available *Acidithiobacillia* class species, and the genome sequences can be confidently aligned on the nucleotide level. So, we selected this group for in-depth analysis of extended type IV loci and CRISPR arrays (Fig. 3 and Supplementary Table S4). The type IV systems in all these genomic islands are located upstream of the genes involved in DNA partitioning during replication (*parA*, *parB*, *dnaN*), in plasmid/ICE DNA rolling circle replication (*uvrD*), and in conjugative DNA transfer (*trbE*, *traG*, *trbI*, *trbG*, *trbF*). The region upstream of the *uvrD*-like gene, containing the type IV *cas* genes, shows signs of instability, with some deletions and insertions (Fig. 3). One such insertion disrupts the *dinG* gene in *F. caldus* MTH-04. Surprisingly, some of the insertions include genes that have not been previously detected in *Fervidacidithiobacillus* and or even the closely related *Acidithiobacillales* (Fig. 3). General context conservation with regional instability extends to other strains of the

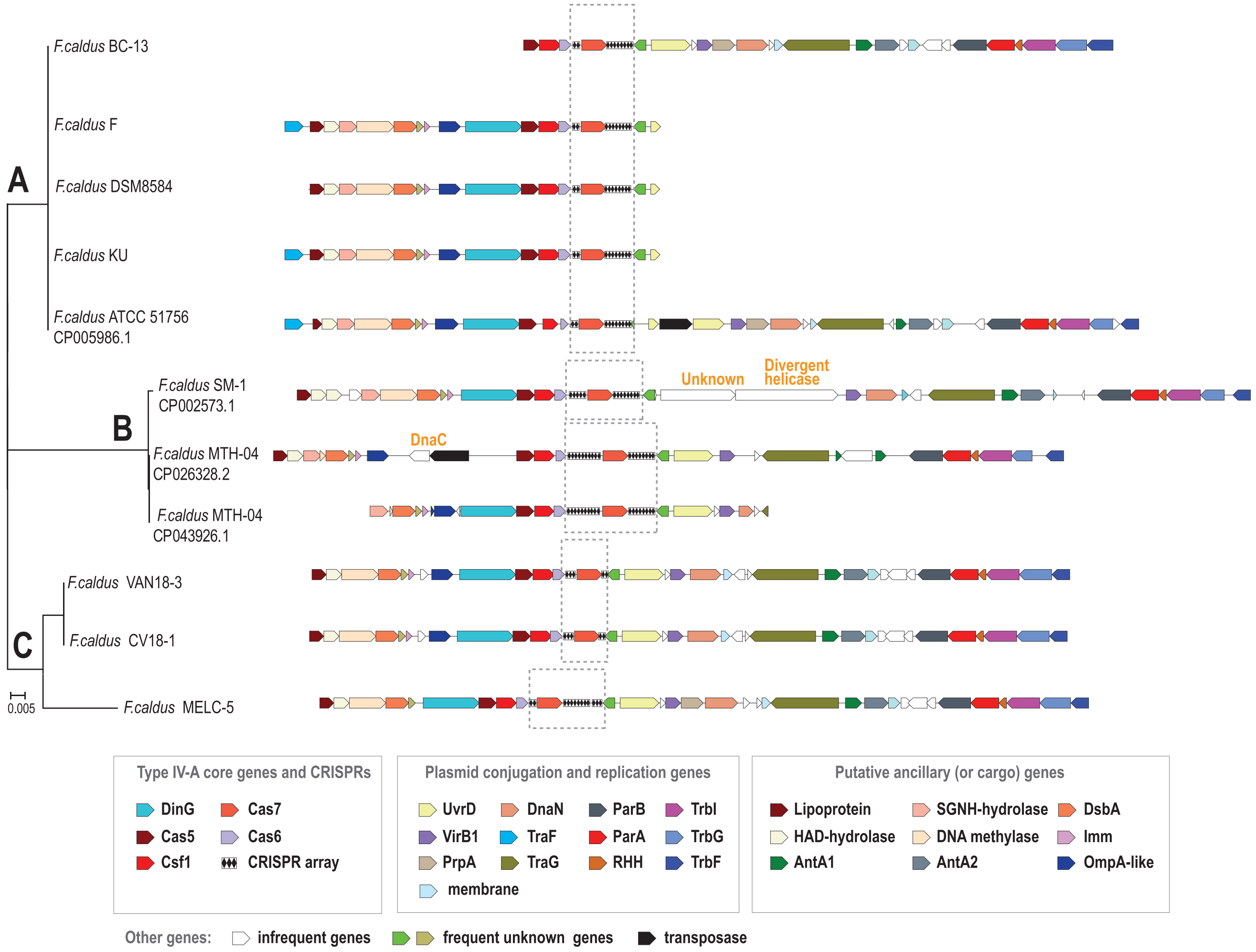

FIG. 3. **(A–C)** Comparative analysis of extended type IV loci in *Fervidacidithiobacillus caldus* strains. The extended type IV-A gene neighborhoods from integrative and conjugative elements from closely related *F. caldus* strains are mapped to the *cas6* nucleotide sequence-based tree, which was constructed using FastTree. The designations are the same as in the Figure 1. The color key and names or short descriptions of the respective genes are given underneath the schematic. A few rare genes that were inserted in the closest vicinity of type IV genes are indicated in *orange* above the respective *blank arrows*. *Gray dashed lines* indicate the regions that are aligned in Supplementary Figure S7.

species (Supplementary Table S3). For example, two genes encoding very large proteins (AEK57865.1, 1,328 aa; AEK57866.1, 971 aa) were inserted in place of the *uvrD* gene in *F. caldus* SM-1, CP002573.1 (Fig. 3). One of these genes encodes a highly diverged helicase, whereas the other one shows no similarity with known protein families. The closest homologs of both proteins were detected in cyanobacteria (as indicated by top scoring hits in BLAST searches; WP_009786411.1: e-value 5e-41, 26.01% identity and WP_137908226.1: e-value 1e-07, 21.61% identity, respectively).

Specific functions of most of these genes are unclear, although they typically belong to known large protein families, such as HAD and alpha/beta superfamily hydrolases, and DsbA-like thioredoxins. However, a potential functional clue comes from the observation that these genes form a putative operon with the gene coding for the superinfection immunity protein Imm (Fig. 3). This membrane protein has been identified and functionally studied in the T4 bacteriophage, and has been shown to inhibit, directly or indirectly, phage DNA injection into the host cell, so that deletion of the *imm* gene resulted in a phage unable to protect cells from superinfection.[50]

Therefore, it seems plausible that all the genes between the lipoprotein and subtype IV-A CRISPR-Cas are involved in functions related to plasmid competition and anti-defense response, clustering together in defense islands similarly to other recently described anti-MGEs genes.[51–53]

Polymorphic repeats in type IV CRISPR arrays of the Acidithiobacillia

To explore the evolution of arrays and spacer acquisition dynamics, we analyzed the CRISPR arrays located upstream and/or downstream of the *csf2* (*cas7*) gene (Fig. 3 and Supplementary Fig. S8). A tree was built from the alignment of the *cas6* nucleotide sequences in order to determine the relationships between the type IV loci in the ''Caldus group'' (Fig. 3). In this case, the tree based on the alignment of the *cas7* nucleotide sequences had the exact same topology as the *cas6* tree (Supplementary Fig. S9). The three branches of this tree (A, B, and C) include five, three, and three loci, respectively. All the sequences of the entire region within the A branch were identical, but the spacer sequences differed between branches A and C, suggestive of an active process of spacer acquisition. Transcriptional expression of the A-branch loci components from representative strains (*F. caldus* ATCC 51756/ DSM 8584) has been demonstrated by RT-PCR, quantitative RT-PCR, and/or RNASeq under diverse growth conditions, being most prominent in attached cells (3–6 × higher) during biofilm formation (Fig. 4 and Supplementary Fig. S10).

To compare repeat and spacer sequences, we clustered them as follows: repeats were joined in a cluster if they were identical, and spacers were clustered if they were at least 90% identical. This clustering revealed a complex picture of array evolution. The 125 repeats in these loci fell into 42 clusters of identical sequences, demonstrating remarkable heterogeneity of repeats within arrays (Fig. 5A and Supplementary Table S4). Typically, different repeats contain several nucleotide substitutions compared to the consensus while retaining the palindromic structure (Fig. 5B). Identical repeats were often scattered along the arrays, and their location differed in the arrays from different branches in the tree. Such polymorphic repeats have not been observed in CRISPR arrays to date and seem to be poorly compatible with the preferential spacer acquisition from one end of the array, accompanied by repeat propagation, which is typically observed in other CRISPR-Cas types (Fig. 5A). Polymorphism of type IV CRISPR repeats also extends to other *Acidithiobacillia* class species (Supplementary Table S4).

The striking diversity of the repeats observed in the Caldus group prompted us to compare the repeats from type IV arrays with CRISPR arrays of other types in greater detail. We used the previously reported curated set of CRISPR systems[1] and analyzed the arrays for nucleotide substitutions compared with the repeat consensus. This comparison showed a dramatically greater within-array variability of repeats in the type IV arrays compared to the arrays from all other CRISPR-Cas systems (Fig. 5C). Repeat sequence variability in type IV loci does not depend on the presence of adaptation modules (Cas1 and/or Cas2; Fig. 5C). It seems most likely that the repeat variability in type IV arrays is underestimated because short arrays with multiple substitutions are not identifiable by the currently available CRISPR array detection methods. Indeed, arrays were missed in several IV-A loci in *Pseudomonas* plasmid genomes (e.g., *P. aeruginosa* strain S04 90 plasmid, CP011370.1, and *P. aeruginosa* RW109 plasmid 2, LT969521.1) as shown by manual examination of these loci. Spacers with perfect matches to TraY from *P. putida* plasmid pND6-2 and a plasmid integrated in *P. aeruginosa* strain GIMC5019:PA52Ts1 genome were identified in these arrays (Supplementary Fig. S11) in evidence of their functionality. Furthermore, we identified RNAseq data in the SRA archive showing that the IV-A array is expressed in *P. aeruginosa* RW109 during exposure to antibiotics (Supplementary Fig. S11). The lack of arrays in most of the subtype IV-B systems might point to the promiscuity of these systems with respect to the crRNA identity, similar to type III effector complexes. Within the subtype IV-B, only some of the IV-D group loci contain arrays. The repeats in these arrays show much less heterogeneity than those in IV-A arrays (Fig. 5C), but the IV-D sample might be too small for a confident conclusion of a lower variability to be made.

Spacers in Acidithiobacillia *type IV arrays preferentially target plasmids*

The majority of the 75 unique spacers in the *F. caldus* arrays showed no reliable matches to any available sequences, with only six distinct spacers matching other *Acidithiobacillia* chromosomes or plasmids and one matching a both plasmid pACMV2JF-5 from *Acidiphilium multivorum* AIU301 and plasmid pACRY05 from *Acidiphilium cryptum* JF-5 (Fig. 5A and Supplementary Table S4). Notably, the identified protospacers came from genes known to be important for plasmid replication or conjugation, in particular, the *traA* gene from *A. cryptum* JF-5 plasmid pACRY05, *mobA* and a permease encoded in *F. caldus* MNG pTcM1, the intergenic region between *repC* and the primase gene in the pTcM1

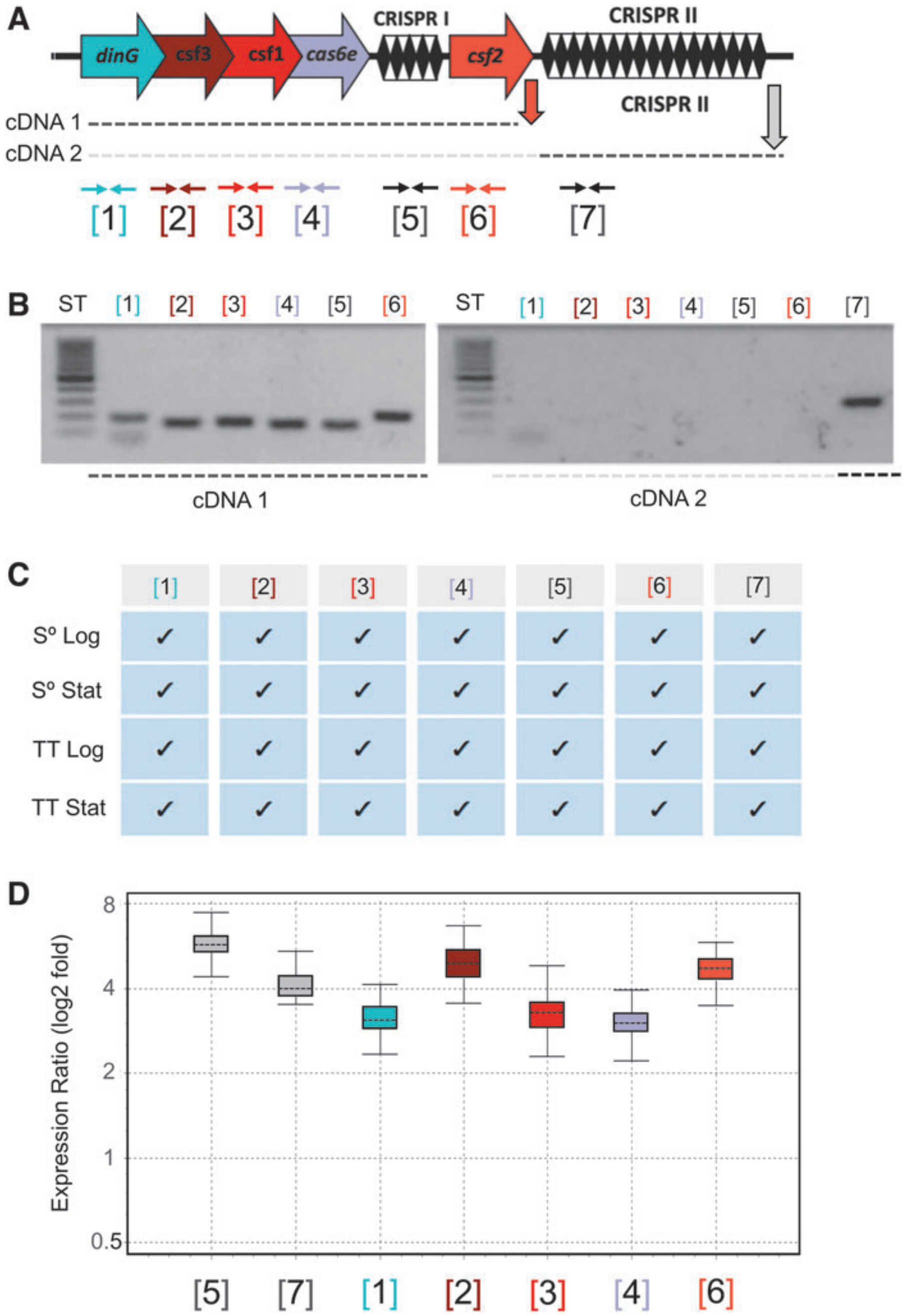

	[1]	[2]	[3]	[4]	[5]	[6]	[7]
S° Log	✓	✓	✓	✓	✓	✓	✓
S° Stat	✓	✓	✓	✓	✓	✓	✓
TT Log	✓	✓	✓	✓	✓	✓	✓
TT Stat	✓	✓	✓	✓	✓	✓	✓

FIG. 4. **(A–D)** Expression of the type IV CRISPR-Cas system of *F. caldus* ATCC 51756^T. Generic scheme showing the *F. caldus* CRISPR-Cas system, the cDNAs obtained by reverse transcription (*dotted lines*), and reverse transcription (RT) polymerase chain reaction (PCR; *vertical arrows*) and PCR primers position (*horizontal arrows*), numbered according to the position of the different features in the loci. Primers used in each reaction are detailed in Supplementary Table S2. **(A)** Analysis of the RT-PCR-amplified products by agarose gel electrophoresis. Total RNA was extracted from mid-log sulfur-grown cultures (pH 2.5; 40°C, 150 rpm; mineral salts medium) and used as template in cDNA synthesis with reverse primers indicated in panel **(A)**. **(B)** Summary of RT-PCR amplification results for total RNA extracted from cells grown under different growth conditions. Cultures were grown in the presence of either sulfur (S°) or tetrathionate (TT) as energy sources, and cells were collected at two distinct growth phases, logarithmic (Log) and stationary (Stat). Positive amplification is indicated by a checkmark. **(C)** Fold induction of each component as assessed by quantitative RT-PCR for total RNA recovered from sessile (biofilm) versus planktonic grown cells (achieved in 6 cm long and 2.5 cm diameter columns containing elemental sulfur-quartz). Gene expression levels in each condition were normalized against a reference gene (*rpoC*, "housekeeping"), and normalized values were used in the calculation of the expression ratio sessile/planktonic.

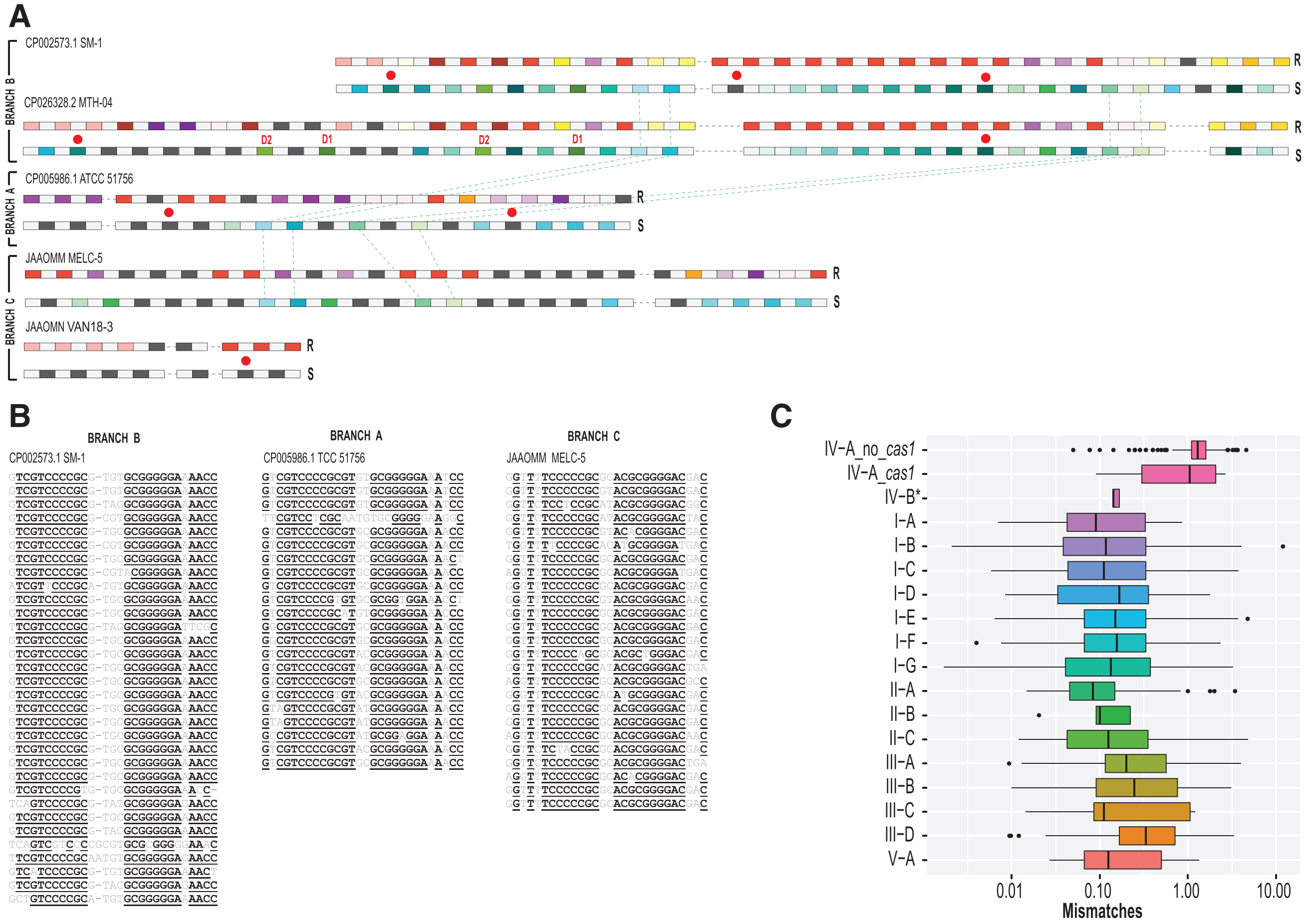

FIG. 5. Comparative analysis of repeats and spacers in *F. caldus* strains and repeat polymorphism in type IV arrays in general. **(A)** CRISPR arrays for five unique loci. For each CRISPR array, two lines representing repeats (*above*) and spacers (*yellow*) are shown. In the first line, repeats (R) are color coded as follows: identical repeats that occur twice or more are shown by *rectangles* of the *same color*, unique repeats are shown by *dark gray rectangles*, and spacers are shown by *light gray rectangles*. In the second line, spacers (S) are color coded as follows: spacers that are 90% identical and occur twice or more are shown by *rectangles* of the *same color*, unique spacers are shown by *dark gray rectangles*, and repeats are shown by *light gray rectangles*. Two parts of CRISPR arrays, upstream and downstream of *csf2* gene and interrupted by insertions, are separated by a dashed line (see Fig. 3). Duplicated spacers are indicated by D1 and D2, respectively. *Red circles* indicate spacers with protospacers identified. *Green dashed lines* indicate spacers common between two branches of the tree shown on the Figure 3. **(B)** Multiple alignments of CRISPR repeats identified in three representative strains from three branches of the tree shown on Figure 3. *Underlined letters* indicate positions with at least 90% identity. **(C)** Number of repeat mismatches for CRISPR arrays per CRISPR-Cas type. The *box plot* shows the weighted average number of repeat mismatches versus repeat consensus per CRISPR array. CRISPR-Cas type indicated on the *y*-axis. For subtype IV-A, the estimates were obtained separately for loci without *cas1* (IV-A_no_*cas1*) and with *cas1* gene (IV-A_*cas1*). The asterisk at IV-B indicates that results were obtained only for a small branch within the subtype IV-B corresponding to the proposed subtype IV-D, where five loci with CRISPR arrays were identified. The remaining IV-B and IV-C arrays were not included because in these loci, arrays are scarce and show a highly patchy distribution (see Fig. 1). The *boxes* show the 25th/50th/75th percentiles, and *black dots* show outliers that fall above 1.5 × interquartile range. For type I, there are ∼10% outliers shown as *dots*.

plasmid from *F. caldus* MNG, and to a chromosomal *trbB* gene from the *F. caldus* type strain genome (pTcM1/pLAtc3) located in a putative ICE region. Interestingly, four spacers are shared by all three branches although surrounded by different repeats (Fig. 4A). Also, in CP026328.2, two spacers are duplicated. Furthermore, considering that *F. caldus* VAN18-3 and CV18-1 group with *F. caldus* MELC-5 (branch C) and *F. caldus* MELC-5 contains an identical region in the arrays with CP005986.1 (branch A), we can conclude that this region was present in the common ancestor of branches C and A, and was deleted from the common ancestor of *F. caldus* VAN18-3 and CV18-1 array (Fig. 3).

In addition to the 75 unique spacers from the *F. caldus* CRISPR loci shown on the Figures 3 and 5, 214 unique spacers were identified in other analyzed *Acidithiobacillia* strains; none of these were similar to those in the Caldus group strains. Among these 214 spacers, only seven had matches in NR and none in the viral database (Supplementary Table S4). At least three of those target ICEs or mobilizable plasmids, which are both common in *Acidithiobacillia* class genomes.[54]

Discussion

The results of in-depth analysis of type IV CRISPR-Cas systems presented here and elsewhere reveal many unusual features of this CRISPR-Cas type. The type IV systems join the expanding group of CRISPR-Cas variants that were recruited by MGE for antidefense and other functions, and in the process of this exaptation, lost their target cleavage activity. In particular, there is a clear parallel between the incorporation of type IV systems in MGE and the recruitment of defective variants of subtype I-B and I-F as well as subtype V-K by Tn7-like transposons, in which these defective CRISPR-Cas systems mediate RNA-guided transposition.[11,55,56]

The origin and directionality of the evolution of type IV systems became more transparent with the identification of subtype IV-C systems and the first structural data on the organization of type IV effector complexes.[1,7,8] These results support the previously proposed hypothesis that type IV systems originated from type III. Many subtype IV-C loci contain no CRISPR array and likely evolved from one of the numerous variants of type III that also lack CRISPR.[1] At the onset of type IV evolution, the large subunit deteriorated, and the HD domain present in the type III and subtype IV-C large subunits was lost, resulting in the loss of the target cleavage capacity, and the minimalist version of the large subunit emerged, giving rise to subtype IV-B. The next major evolutionary event was the origin of subtype IV-A, which evolved by the loss of the small subunit and the recruitment of DinG, possibly, compensating for the absence of the small subunit. CRISPR arrays, Cas6 and, less frequently, adaptation modules were acquired on several independent occasions, mostly by subtype IV-A systems (Fig. 6).

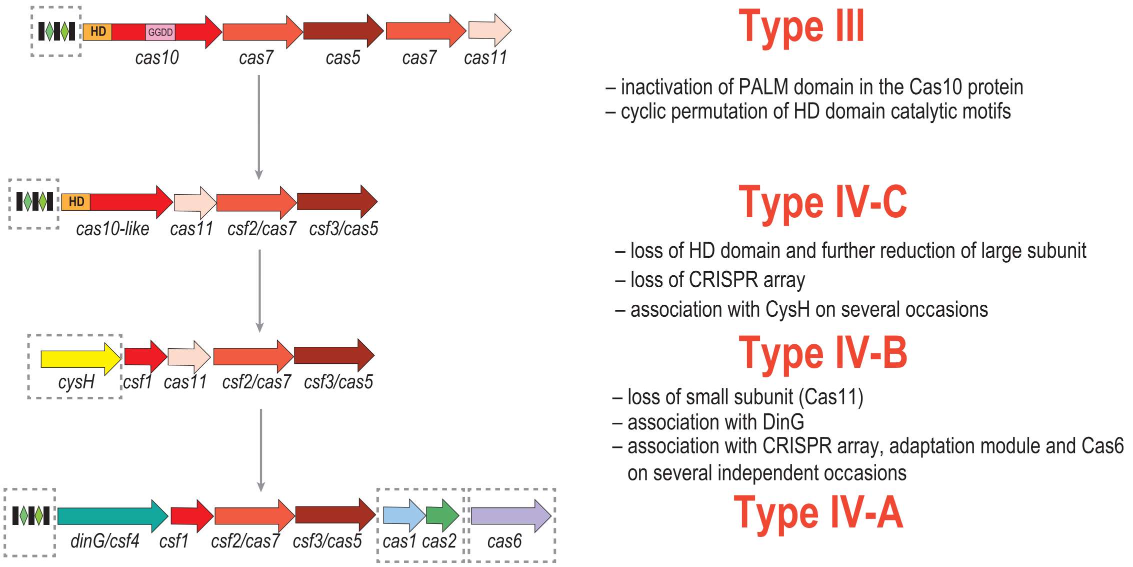
HD
GGDD
cas10
cas7
cas5
cas7
cas11
Type III
– inactivation of PALM domain in the Cas10 protein
– cyclic permutation of HD domain catalytic motifs
HD
cas10-like
cas11
csf2/cas7
csf3/cas5
Type IV-C
– loss of HD domain and further reduction of large subunit
– loss of CRISPR array
– association with CysH on several occasions
cysH
csf1
cas11
csf2/cas7
csf3/cas5
Type IV-B
– loss of small subunit (Cas11)
– association with DinG
– association with CRISPR array, adaptation module and Cas6 on several independent occasions
dinG/csf4
csf1
csf2/cas7
csf3/cas5
cas1
cas2
cas6
Type IV-A

FIG. 6. A hypothetical scenario for the origins of type IV CRISPR-Cas systems. Homologous genes are shown as color-coded *arrows* or *rectangles* (for domains) and identified by a family name. The key evolutionary events are described to the right of the images. Optional genes and CRISPR arrays are denoted by *dashed outlines*. GGDD: key catalytic motif of the cyclase/polymerase domain of Cas10.

Type IV is exceptional among CRISPR-Cas systems in harboring highly polymorphic repeats. The biological underpinning and impact of this within-array repeat heterogeneity remain unclear, but considering that most of the type IV systems lack adaptation genes, it seems possible that they acquire new spacers via recombination between CRISPR arrays encoded on different MGEs rather than via a typical adaptation route. The few *cas1* genes that are associated with type IV loci are monophyletic and originate from type I-E Cas1, with the exception of several type IV loci in *Pseudomonas*, which encode Cas1 apparently originating from subtype I-F. It is of interest whether these Cas1 proteins, especially the former, possess any distinct functional properties, such as an ability to insert new repeats in random positions within the CRISPR array.

Our analysis of the genes that often accompany type IV CRISPR-Cas systems showed that the most common of these genes, *cysH* and *recD/traA*, are frequently present in numerous MGE, not only within type IV CRISPR-Cas loci. However, *cysH* genes associated with subtype IV-B are largely monophyletic, suggesting a strong functional link. Several other functionally uncharacterized genes and apparent modules were also found to be consistently associated with type IV loci (Table 1), but the majority of the neighbors in these loci are highly diverse and belong to the genomic ''dark matter.'' However, analysis of the context of the Caldus group type IV loci, which encode superinfection immunity protein Imm, suggests that type IV systems, along with most of the other genes in the same neighborhoods, belong to ''cargo'' regions of ICEs and other MGE, and are involved in inter-MGE conflicts and, possibly, additional functions in MGE reproduction.

The results of the present analysis seem to provide little or no support for the proposed reclassification of type IV systems. Indeed, in subtype IV-A, the proposed variants A1 and A2 are not monophyletic.[6] Furthermore, all proposed IV-A variants—A1, A2, and A3—share the same set of effector genes, and the sequences of the core genes Csf2 and Csf3 are closely similar. Divergence of large or small subunits of the effector complexes has not been previously considered sufficient reason to reclassify CRISPR-Cas subtypes (e.g., in subtype I-B, there are 13 distinct large subunits that share no detectable sequence similarity), and the proposed variants lack any other features that would suggest major functional differences. The proposed subtype IV-E shares the same set of effector complex genes and the ancillary gene *dinG* with subtype IV-A, and the fusion of the effector genes generally is not thought to justify establishing a new subtype. The E branch confidently groups with type IV-A in the Cas7 and Cas5 trees, and all the E loci encode DinG, the signature of subtype IV-A. Thus, we believe that this subfamily should remain within type IV-A.

The proposed subtype D is the most notable type IV variant. Our analysis suggests that this is a hybrid system, with Csf2 (Cas7) and the large subunit Csf1 originating from within the IV-B clade, whereas Csf3 (Cas5) is from the IV-A clade. The *Csf1* and *Csf3* genes are not monophyletic and apparently became independently associated with Csf2 at least twice. Most of the IV-D systems are encoded in predicted operons, together with a gene coding for a RecD/TraA family helicase. This association also appears to have evolved independently on at least three occasions. However, *recD/traA* genes are also found in extended loci of other systems, such as subtype IV-A. These chimeric loci present a challenge for the current classification approach. There seems to be no compelling reason to classify these loci as a separate subtype given the apparent polyphyly of all the components of the proposed IV-D system, and we therefore propose to classify these systems as type IV-B based on the Cas7 (Csf2) phylogeny. Otherwise, all the distinguishing features that were used to classify type IV systems into the A and B subtypes remain valid. So, we propose adhering to this classification, ahead of additional comparative genomic and experimental evidence that might call for modifications to the classification scheme.

Many outstanding questions regarding the functions of type IV systems remain to be answered. In particular, the source of the crRNA for type IV-B systems lacking CRISPR arrays remains to be identified. Most significantly, the specific role and the mechanism of the involvement of type IV systems in MGE interference and possibly other processes are currently unclear, and the functions of the associated genes, such as *dinG*, *cysH*, *recD*, and others, have also to be elucidated.

Acknowledgment

R.Q. would like to acknowledge J.F. Banfield for her contributions and inspiration at early stages of the analysis the type IV CRIPSR-Cas loci in the *Acidithiobacillia* class representatives.

Author Disclosure Statement

No competing financial interests exist.

Funding Information

K.S.M., Y.I.W., S.A.S., I.T., and E.V.K. are supported by the Intramural Research Program of the National Institutes of Health of the USA (National Library of Medicine). This work was supported the Agencia Nacional de Investigación y Desarrollo (ANID, Chile) under Grants FONDECYT 1181251 (R.Q.), FONDECYT 11201070

(L.G.A.), Programa de Apoyo a Centros con Financiamiento Basal AFB170004 (R.Q.), CONICYT-PFCHA/Doctorado Nacional/20171049 (A.M.-B.), CONICYT-PFCHA/Doctorado Nacional/21090398 (L.G.A.), CONICYT-PFCHA/Doctorado Nacional/21120305 (P.C.C.), CONICYT/FONDAP Grant No. 15110027 (L.G.A.), and the ANID—Millennium Science Initiative Programme—NCN17_093, granted by the Ministry of Economy, Development and Tourism from Chile (R.Q.).

Supplementary Material

Supplementary Figure S1
Supplementary Figure S2
Supplementary Figure S3
Supplementary Figure S4
Supplementary Figure S5
Supplementary Figure S6
Supplementary Figure S7
Supplementary Figure S8
Supplementary Figure S9
Supplementary Figure S10
Supplementary Figure S11
Supplementary Table S1
Supplementary Table S2
Supplementary Table S3
Supplementary Table S4

References

1. Makarova KS, Wolf YI, Iranzo J, et al. Evolutionary classification of CRISPR-Cas systems: a burst of class 2 and derived variants. *Nat Rev Microbiol* 2020;18:67–83. DOI: 10.1038/s41579-019-0299-x.
2. Makarova KS, Haft DH, Barrangou R, et al. Evolution and classification of the CRISPR-Cas systems. *Nat Rev Microbiol* 2011;9:467–477. DOI: 10.1038/nrmicro2577.
3. Bustamante P, Covarrubias PC, Levican G, et al. ICE Afe 1, an actively excising genetic element from the biomining bacterium *Acidithiobacillus ferrooxidans*. *J Mol Microbiol Biotechnol* 2012;22:399–407. DOI: 10.1159/000346669.
4. Quatrini R, Johnson DB. *Acidithiobacillus ferrooxidans*. *Trends Microbiol* 2019;27:282–283. DOI: 10.1016/j.tim.2018.11.009.
5. Valdes J, Pedroso I, Quatrini R, et al. *Acidithiobacillus ferrooxidans* metabolism: from genome sequence to industrial applications. *BMC Genomics* 2008;9:597. DOI: 10.1186/1471-2164-9-597.
6. Pinilla-Redondo R, Mayo-Munoz D, Russel J, et al. Type IV CRISPR-Cas systems are highly diverse and involved in competition between plasmids. *Nucleic Acids Res* 2020;48:2000–2012. DOI: 10.1093/nar/gkz1197.
7. Ozcan A, Pausch P, Linden A, et al. Type IV CRISPR RNA processing and effector complex formation in *Aromatoleum aromaticum*. *Nat Microbiol* 2019;4:89–96. DOI: 10.1038/s41564-018-0274-8.
8. Zhou Y, Bravo JPK, Taylor HN, et al. Structure of a type IV CRISPR-Cas ribonucleoprotein complex. *iScience* 2021;24:102201.
9. Makarova KS, Aravind L, Wolf YI, et al. Unification of Cas protein families and a simple scenario for the origin and evolution of CRISPR-Cas systems. *Biol Direct* 2011;6:38. DOI: 10.1186/1745-6150-6-38.
10. Shmakov SA, Makarova KS, Wolf YI, et al. Systematic prediction of genes functionally linked to CRISPR-Cas systems by gene neighborhood analysis. *Proc Natl Acad Sci U S A* 2018;115:E5307–E5316. DOI: 10.1073/pnas.1803440115.
11. Faure G, Shmakov SA, Yan WX, et al. CRISPR-Cas in mobile genetic elements: counter-defence and beyond. *Nat Rev Microbiol* 2019;17:513–525. DOI: 10.1038/s41579-019-0204-7.
12. Newire E, Aydin A, Juma S, et al. Identification of a type IV-A CRISPR-Cas system located exclusively on IncHI1B/IncFIB plasmids in *Enterobacteriaceae*. *Front Microbiol* 2020;11:1937. DOI: 10.3389/fmicb.2020.01937.
13. Kamruzzaman M, Iredell JR. CRISPR-Cas system in antibiotic resistance plasmids in *Klebsiella pneumoniae*. *Front Microbiol* 2019;10:2934. DOI: 10.3389/fmicb.2019.02934.
14. Taylor HN, Warner EE, Armbrust MJ, et al. Structural basis of Type IV CRISPR RNA biogenesis by a Cas6 endoribonuclease. *RNA Biol* 2019;16:1438–1447. DOI: 10.1080/15476286.2019.1634965.
15. Crowley VM, Catching A, Taylor HN, et al. A type IV-A CRISPR-Cas system in *Pseudomonas aeruginosa* mediates RNA-guided plasmid interference *in vivo*. *CRISPR J* 2019;2:434–440. DOI: 10.1089/crispr.2019.0048.
16. Acuna LG, Cardenas JP, Covarrubias PC, et al. Architecture and gene repertoire of the flexible genome of the extreme acidophile *Acidithiobacillus caldus*. *PLoS One* 2013;8:e78237. DOI: 10.1371/journal.pone.0078237.
17. Moya-Beltran A, Beard S, Rojas-Villalobos C, et al. Genomic evolution of the class *Acidithiobacillia*: deep-branching *Proteobacteria* living in extreme acidic conditions. *ISME J* 2021 May 18 [Epub ahead of print]; DOI: 10.1038/s41396-021-00995-x.
18. Altschul SF, Madden TL, Schaffer AA, et al. Gapped BLAST and PSI-BLAST: a new generation of protein database search programs. *Nucleic Acids Res* 1997;25:3389–3402.
19. Marchler-Bauer A, Zheng C, Chitsaz F, et al. CDD: conserved domains and protein three-dimensional structure. *Nucleic Acids Res* 2013;41:D348–352. DOI: 10.1093/nar/gks1243.
20. Soding J. Protein homology detection by HMM-HMM comparison. *Bioinformatics* 2005;21:951–960. DOI: 10.1093/bioinformatics/bti125.
21. Russel J, Pinilla-Redondo R, Mayo-Munoz D, et al. CRISPRCasTyper: automated identification, annotation, and classification of CRISPR-Cas loci. *CRISPR J* 2020;3:462–469. DOI: 10.1089/crispr.2020.0059.
22. Bland C, Ramsey TL, Sabree F, et al. CRISPR recognition tool (CRT): a tool for automatic detection of clustered regularly interspaced palindromic repeats. *BMC Bioinformatics* 2007;8:209. DOI: 10.1186/1471-2105-8-209.
23. Grissa I, Vergnaud G, Pourcel C. CRISPRFinder: a web tool to identify clustered regularly interspaced short palindromic repeats. *Nucleic Acids Res* 2007;35:W52–57. DOI: 10.1093/nar/gkm360.
24. Biswas A, Gagnon JN, Brouns SJ, et al. CRISPRTarget: bioinformatic prediction and analysis of crRNA targets. *RNA Biol* 2013;10:817–827. DOI: 10.4161/rna.24046.
25. Steinegger M, Soding J. MMseqs2 enables sensitive protein sequence searching for the analysis of massive data sets. *Nat Biotechnol* 2017;35:1026–1028. DOI: 10.1038/nbt.3988.
26. Edgar RC. MUSCLE: multiple sequence alignment with high accuracy and high throughput. *Nucleic Acids Res* 2004;32:1792–1797.
27. Nguyen LT, Schmidt HA, von Haeseler A, et al. IQ-TREE: a fast and effective stochastic algorithm for estimating maximum-likelihood phylogenies. *Mol Biol Evol* 2015;32:268–274. DOI: 10.1093/molbev/msu300.
28. Price MN, Dehal PS, Arkin AP. FastTree 2—approximately maximum-likelihood trees for large alignments. *PLoS One* 2010;5:e9490. DOI: 10.1371/journal.pone.0009490.
29. Katoh K, Standley DM. MAFFT multiple sequence alignment software version 7: improvements in performance and usability. *Mol Biol Evol* 2013;30:772–780. DOI: 10.1093/molbev/mst010.
30. Nieto PA, Covarrubias PC, Jedlicki E, et al. Selection and evaluation of reference genes for improved interrogation of microbial transcriptomes: case study with the extremophile *Acidithiobacillus ferrooxidans*. *BMC Mol Biol* 2009;10:63. DOI: 10.1186/1471-2199-10-63.
31. Bick JA, Dennis JJ, Zylstra GJ, et al. Identification of a new class of 5′-adenylylsulfate (APS) reductases from sulfate-assimilating bacteria. *J Bacteriol* 2000;182:135–142. DOI: 10.1128/jb.182.1.135-142.2000.
32. Xiong L, Liu S, Chen S, et al. A new type of DNA phosphorothioation-based antiviral system in archaea. *Nat Commun* 2019;10:1688. DOI: 10.1038/s41467-019-09390-9.
33. Xu T, Yao F, Zhou X, et al. A novel host-specific restriction system associated with DNA backbone S-modification in *Salmonella*. *Nucleic Acids Res* 2010;38:7133–7141. DOI: 10.1093/nar/gkq610.
34. Farlow J, Bolkvadze D, Leshkasheli L, et al. Genomic characterization of three novel Basilisk-like phages infecting *Bacillus anthracis*. *BMC Genomics* 2018;19:685. DOI: 10.1186/s12864-018-5056-4.
35. Garcia P, Monjardin C, Martin R, et al. Isolation of new *Stenotrophomonas* bacteriophages and genomic characterization of temperate phage S1. *Appl Environ Microbiol* 2008;74:7552–7560. DOI: 10.1128/AEM.01709-08.

36. Summer EJ, Gill JJ, Upton C, et al. Role of phages in the pathogenesis of *Burkholderia*, or "Where are the toxin genes in *Burkholderia* phages?" *Curr Opin Microbiol* 2007;10:410–417. DOI: 10.1016/j.mib.2007.05.016.
37. Kopriva S, Koprivova A. Plant adenosine 5′-phosphosulphate reductase: the past, the present, and the future. *J Exp Bot* 2004;55:1775–1783. DOI: 10.1093/jxb/erh185.
38. Taylor HN, Laderman E, Armbrust M, et al. Positioning diverse type IV structures and functions within class 1 CRISPR-Cas systems. *Front Microbiol* 2021;12:671522. DOI: 10.3389/fmicb.2021.671522.
39. Yang JC, Lessard PA, Sengupta N, et al. TraA is required for megaplasmid conjugation in *Rhodococcus erythropolis* AN12. *Plasmid* 2007;57:55–70. DOI: 10.1016/j.plasmid.2006.08.002.
40. Rogozin IB, Makarova KS, Wolf YI, et al. Computational approaches for the analysis of gene neighbourhoods in prokaryotic genomes. *Brief Bioinform* 2004;5:131–149. DOI: 10.1093/bib/5.2.131.
41. Dyson ZA, Tucci J, Seviour RJ, et al. Isolation and characterization of bacteriophage SPI1, which infects the activated-sludge-foaming bacterium *Skermania piniformis*. *Arch Virol* 2016;161:149–158. DOI: 10.1007/s00705-015-2631-8.
42. Bignell C, Thomas CM. The bacterial ParA-ParB partitioning proteins. *J Biotechnol* 2001;91:1–34. DOI: S0168165601002930.
43. Castillo F, Benmohamed A, Szatmari G. Xer site specific recombination: double and single recombinase systems. *Front Microbiol* 2017;8:453. DOI: 10.3389/fmicb.2017.00453.
44. Kaur G, Burroughs AM, Iyer LM, et al. Highly regulated, diversifying NTP-dependent biological conflict systems with implications for the emergence of multicellularity. *Elife* 2020;9. DOI: 10.7554/eLife.52696.
45. Flores-Rios R, Moya-Beltran A, Pareja-Barrueto C, et al. The type IV secretion system of ICEAfe1: formation of a conjugative pilus in *Acidithiobacillus ferrooxidans*. *Front Microbiol* 2019;10:30. DOI: 10.3389/fmicb.2019.00030.
46. Cabezon E, Ripoll-Rozada J, Pena A, et al. Towards an integrated model of bacterial conjugation. *FEMS Microbiol Rev* 2015;39:81–95. DOI: 10.1111/1574-6976.12085.
47. Guglielmini J, Quintais L, Garcillan-Barcia MP, et al. The repertoire of ICE in prokaryotes underscores the unity, diversity, and ubiquity of conjugation. *PLoS Genet* 2011;7:e1002222. DOI: 10.1371/journal.pgen.1002222.
48. Wozniak RA, Waldor MK. Integrative and conjugative elements: mosaic mobile genetic elements enabling dynamic lateral gene flow. *Nat Rev Microbiol* 2010;8:552–563. DOI: 10.1038/nrmicro2382.
49. Moya-Beltran A, Rojas-Villalobos C, Diaz M, et al. Nucleotide second messenger-based signaling in extreme acidophiles of the *Acidithiobacillus* species complex: partition between the core and variable gene complements. *Front Microbiol* 2019;10:381. DOI: 10.3389/fmicb.2019.00381.
50. Lu MJ, Henning U. The immunity (imm) gene of *Escherichia coli* bacteriophage T4. *J Virol* 1989;63:3472–3478. DOI: 10.1128/JVI.63.8.3472-3478.1989.
51. Koonin EV, Zhang F. Coupling immunity and programmed cell suicide in prokaryotes: life-or-death choices. *Bioessays* 2017;39:1–9. DOI: 10.1002/bies.201600186.
52. Makarova KS, Wolf YI, Snir S, et al. Defense islands in bacterial and archaeal genomes and prediction of novel defense systems. *J Bacteriol* 2011;193:6039–6056. DOI: 10.1128/JB.05535-11.
53. Doron S, Melamed S, Ofir G, et al. Systematic discovery of antiphage defense systems in the microbial pangenome. *Science* 2018;359. DOI: 10.1126/science.aar4120.
54. Beard S, Ossandon FJ, Rawlings DE, et al. The flexible genome of acidophilic prokaryotes. *Curr Issues Mol Biol* 2021;40:231–266. DOI: 10.21775/cimb.040.231.
55. Klompe SE, Vo PLH, Halpin-Healy TS, et al. Transposon-encoded CRISPR-Cas systems direct RNA-guided DNA integration. *Nature* 2019;571:219–225. DOI: 10.1038/s41586-019-1323-z.
56. Strecker J, Ladha A, Gardner Z, et al. RNA-guided DNA insertion with CRISPR-associated transposases. *Science* 2019;365:48–53. DOI: 10.1126/science.aax9181.
57. Makarova KS, Wolf YI, Koonin EV. Classification and nomenclature of CRISPR-Cas systems: where from here? *CRISPR J* 2018;1:325–336. DOI: 10.1089/crispr.2018.0033.
58. Makarova KS, Wolf YI, Shmakov SA, et al. Unprecedented diversity of unique CRISPR-Cas-related systems and Cas1 homologs in *Asgard* archaea. *CRISPR J* 2020;3:156–163. DOI: 10.1089/crispr.2020.0012.
59. Chartron J, Carroll KS, Shiau C, et al. Substrate recognition, protein dynamics, and iron-sulfur cluster in *Pseudomonas aeruginosa* adenosine 5′-phosphosulfate reductase. *J Mol Biol* 2006;364:152–169. DOI: 10.1016/j.jmb.2006.08.080.
60. Buetti-Dinh A, Herold M, Christel S, et al. Systems biology of acidophile biofilms for efficient metal extraction. *Sci Data* 2020;7:215. DOI: 10.1038/s41597-020-0519-2.